iScience

CellPress
OPEN ACCESS

Article

Selective modulator of nuclear receptor PPARγ with reduced adipogenic potential ameliorates experimental nephrotic syndrome

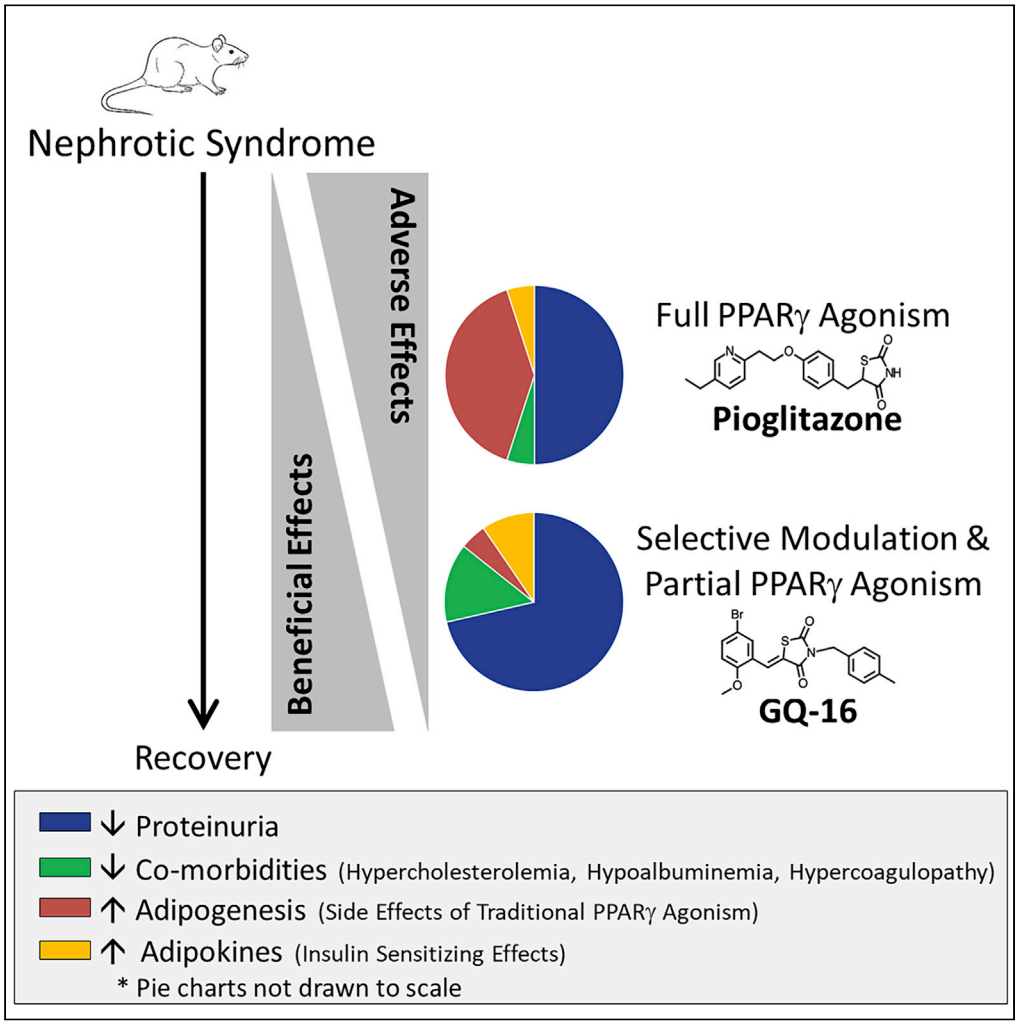

Claire Bryant, Galen Rask, Amanda P. Waller, ..., Francisco A.R. Neves, Alessia Fornoni, Shipra Agrawal

shipra.agrawal@nationwidechildrens.org

Highlights

Selective Modulation of PPARγ offers therapeutic advantage over full agonism in NS

GQ-16 reduces proteinuria in NS and associated comorbidities with high efficacy

RNA-Seq identified common and distinct glomerular gene expression by GQ-16 and pioglitazone

Pioglitazone induces more markers of adipogenesis, and GQ-16 induces adipokines to a greater degree

Bryant et al., iScience 25, 104001
April 15, 2022
https://doi.org/10.1016/j.isci.2022.104001

iScience

CellPress
OPEN ACCESS

Article

Selective modulator of nuclear receptor PPARγ with reduced adipogenic potential ameliorates experimental nephrotic syndrome

Claire Bryant,[1] Galen Rask,[1] Amanda P. Waller,[1] Amy Webb,[2] Marina R. Galdino-Pitta,[3] Angelica A. Amato,[4] Rachel Cianciolo,[5] Rajgopal Govindarajan,[6] Brian Becknell,[1,7] Bryce A. Kerlin,[1,7] Francisco A.R. Neves,[4] Alessia Fornoni,[8] and Shipra Agrawal[1,7,9,*]

SUMMARY

Glomerular disease manifests as nephrotic syndrome (NS) with high proteinuria and comorbidities, and is frequently refractory to standard treatments. We hypothesized that a selective modulator of PPARγ, GQ-16, will provide therapeutic advantage over traditional PPARγ agonists for NS treatment. We demonstrate in a pre-clinical NS model that proteinuria is reduced with pioglitazone to 64%, and robustly with GQ-16 to 81% of nephrosis, comparable to controls. Although both GQ-16 and pioglitazone restore glomerular-*Nphs1*, hepatic-*Pcsk9* and serum-cholesterol, only GQ-16 restores glomerular-*Nrf2*, and reduces hypoalbuminemia and hypercoagulopathy. GQ-16 and pioglitazone restore common and distinct glomerular gene expression analyzed by RNA-seq and induce insulin sensitizing adipokines to various degrees. Pioglitazone but not GQ-16 induces more lipid accumulation and *aP2* in adipocytes and white adipose tissue. We conclude that selective modulation of PPARγ by a partial agonist, GQ-16, is more advantageous than pioglitazone in reducing proteinuria, NS associated comorbidities, and adipogenic side effects of full PPARγ agonists.

INTRODUCTION

Various forms of glomerular disease, manifesting as nephrotic syndrome (NS) with high-grade proteinuria, can be frequently refractory to treatment leading to progression to chronic kidney disease and end-stage kidney disease (ESKD) (Floege et al., 2019; Luyckx et al., 2018; Rovin et al., 2019). Moreover, NS is typically associated with edema, hypercholesterolemia, hypoalbuminemia, systemic immune dysregulation, and hypercoagulopathy (Agrawal et al., 2018; Araya et al., 2006, 2009; Radhakrishnan, 2020; Siddall and Radhakrishnan, 2012). To identify alternate effective treatments for glomerular disease, we and others have previously reported that peroxisome proliferator-activated receptor γ (PPARγ) agonists and thiazolidinediones (TZDs) such as pioglitazone (Pio), directly protect podocytes from injury (Agrawal et al., 2011; Kanjanabuch et al., 2007; Miglio et al., 2011, 2012) and reduce proteinuria and glomerular injury in various animal models of glomerular disease (Agrawal et al., 2016, 2021; Henique et al., 2016; Ma et al., 2001; Platt and Coward, 2016; Sonneveld et al., 2017; Yang et al., 2006, 2009; Zuo et al., 2012). They have also been shown to improve clinical outcomes in NS patients refractory to steroid treatment (Agrawal et al., 2016; Hunley et al., 2019). Moreover, these protective effects in experimental models have been shown to be mediated by activation of podocyte PPARγ, indicating an essential role for PPARγ in maintaining glomerular function through the preservation of podocytes even in non-diabetic glomerular diseases in addition to their beneficial metabolic, insulin-sensitizing and anti-inflammatory effects (Agrawal et al., 2016, 2021; Henique et al., 2016; Sonneveld et al., 2017).

Since the identification of PPARs in 1990, PPARγ has been recognized as a nuclear receptor superfamily member, a ligand-dependent transcription factor, and a master regulator of adipogenesis and metabolism. The ability of PPARγ to regulate lipid storage and adipogenesis accounts for the insulin-sensitizing effects of its agonists or anti-diabetic drugs known as TZDs (Heikkinen et al., 2007). Interestingly, in a meta analyses study in patients with diabetes mellitus and diabetic nephropathy (DN), TZDs have been shown to exhibit antiproteinuric effects and a decrease in urinary podocyte loss (Nakamura et al., 2001; Sarafidis

[1]Center for Clinical and Translational Research, Abigail Wexner Research Institute at Nationwide Children's Hospital, Columbus, OH, USA

[2]The Ohio State University, Department of Biomedical Informatics, Columbus, OH, USA

[3]Laboratory of Design and Drug Synthesis, Bioscience Center, Federal University of Pernambuco, Recife, Brazil

[4]Laboratório de Farmacologia Molecular, Departamento de Ciências Farmacêuticas, Faculdade de Ciências da Saúde, Universidade de Brasília, Brasilia, Brazil

[5]Deptartment of Veterinary Biosciences, The Ohio State University, Columbus, OH, USA

[6]Division of Pharmaceutics and Pharmacology, College of Pharmacy, The Ohio State University, Columbus, OH, USA

[7]Department of Pediatrics, College of Medicine, The Ohio State University, Columbus, OH, USA

[8]Katz Family Division of Nephrology and Hypertension, Peggy and Harold Katz Drug Discovery Center, University of Miami Miller School of Medicine, Miami, FL, USA

[9]Lead contact

*Correspondence: shipra.agrawal@nationwidechildrens.org

https://doi.org/10.1016/j.isci.2022.104001

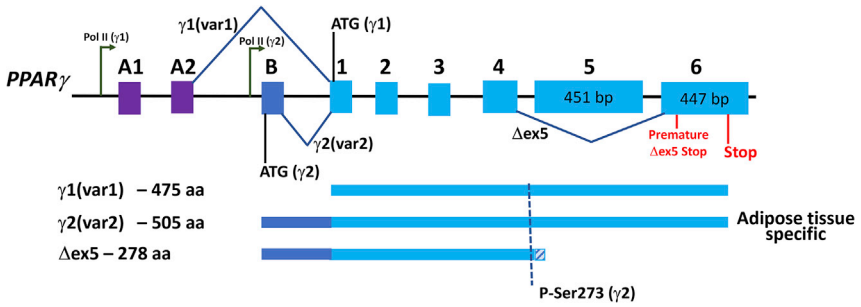

Figure 1. PPARγ isoforms and phosphorylation site

PPARγ exists in mainly two major isoforms, γ1 and γ2, which are a result of different promoter usage by RNA Polymerase II (depicted in tall arrows) and alternative splicing (depicted by exon skipping), resulting in variants 1 and 2. Although γ1 variant 1 includes exons A1 and A2 upstream of the start codon (ATG) on exon 1, γ2 variant 2 contains the transcription start site preceding exon B and initiates translation on the start codon (ATG) in exon B, resulting in γ2 protein product, which is 30 amino acids longer than γ1. In a relatively unexplored variant that skips exon 5 (Δex5), a frameshift occurs on exon 6 because of exon 5 being spliced out, which creates a premature stop codon. One of the major sites of phosphorylation on Serine 273 (Ser273) is depicted. This is coded by the last codon on exon 4, thus it remains conserved in variant1, variant 2, and Δex5. The relative position of Ser273 is changed to Ser243 in the isoform γ1. This figure depicts the human annotations for variants 1 (var1: GenBank: NM_138712) and 2 (var2: GenBank: NM_015869) encoding isoforms γ1 and γ2. These variants and isoforms correspond to reversed numbers in rat and are annotated as 2 (var2: GenBank: NM_001145366) and 1 (var1: GenBank: NM_013124), respectively.

et al., 2010). In addition, PPARγ exists in both tissue- and function-specific forms which can be generated due to alternative splicing, promoter usage (Fajas et al., 1997; Mukherjee et al., 1997), and its differential phosphorylation, specifically at serine (Ser) 273 (Choi et al., 2011; Hall et al., 2020), which have been shown to be important determinants of its effects on adipogenesis and insulin sensitivity (Figure 1). However, the roles of these determinants in glomerular disease are unexplored.

Targeting PPARγ with widely marketed anti-diabetic drugs, the TZDs Pio and especially rosiglitazone, has recently been under scrutiny because of reported side effects such as weight gain, increased risk of edema, heart failure, bone loss, and bladder cancer (Friedland et al., 2012; Nesto et al., 2003; Nissen and Wolski, 2007; Tang et al., 2018; Viscoli et al., 2017; Yki-Jarvinen, 2004). More recently, breakthrough discoveries in the field of PPARγ biology have led to the generation of a series of novel compounds with a weak traditional PPARγ agonistic activity (adipogenic), but very good anti-diabetic activity (Amato et al., 2012; Choi et al., 2010, 2011; Coelho et al., 2016). GQ-16, a novel selective modulator of PPARγ has been demonstrated to improve insulin sensitivity in diabetic mice in the absence of weight gain and edema (Amato et al., 2012; Coelho et al., 2016). Moreover, GQ-16 treatment is accompanied by reduced activation of *aP2* and lipid accumulation *in vitro* and induction of thermogenesis-related genes in epididymal fat depots *in vivo*, suggesting that browning of visceral white adipose tissue (WAT) may have contributed to weight loss (Amato et al., 2012; Coelho et al., 2016). This advantageous pharmacological profile appears to be because of the unique binding mode of GQ-16 to PPARγ and stabilization of beta sheets, which is distinct from traditional TZDs (Amato et al., 2012; Coelho et al., 2016).

Based on the above, we hypothesized that the downstream effects of PPARγ can be mechanistically dissociated and that selected manipulation of PPARγ by a novel partial agonist, GQ-16, will result in a better and targeted therapeutic advantage in glomerular disease. To test this hypothesis, we analyzed the abilities of GQ-16 and Pio to: 1) provide reduction in proteinuria and glomerular injury, 2) regulate systemic and adipogenic effects by complete vs. partial agonism of PPARγ, and 3) modulate downstream molecular pathways, in an animal model of glomerular disease.

RESULTS

GQ-16 activates PPARγ partially and reduces proteinuria and hypoalbuminemia in a rat model of PAN-induced nephropathy

To assess the efficacy of GQ-16 and to compare it with a traditional agonist of PPARγ, Pio, in reducing proteinuria in a glomerular disease model, a puromycin aminonucleoside (PAN)-induced nephropathy model was utilized. Efficacy of PPARγ activation was first measured and compared *in vitro* using a luciferase assay system. In agreement with previous data, GQ-16 displayed partial PPARγ agonist activity in

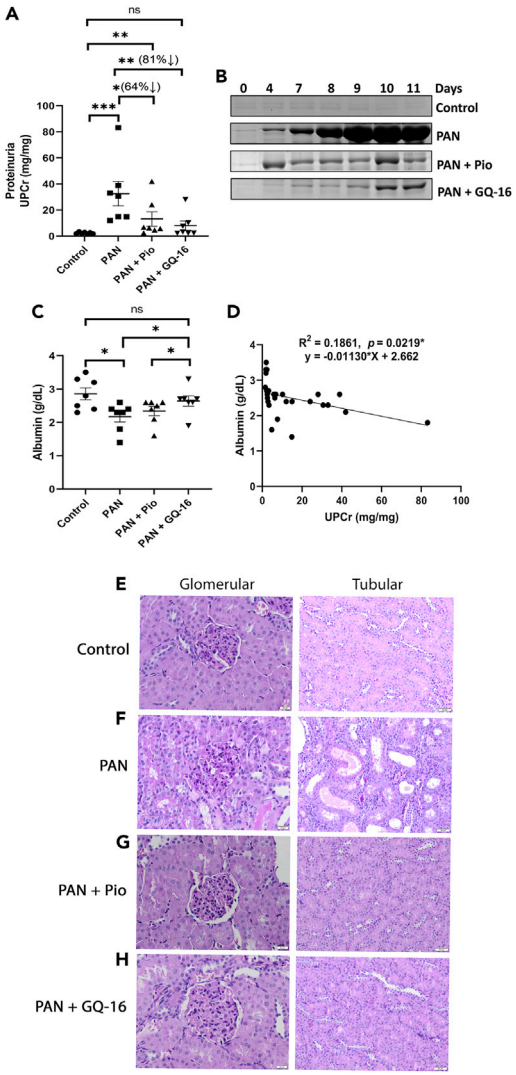

Figure 2. GQ-16 reduces proteinuria and hypoalbuminemia in a rat model of PAN-induced nephropathy

Proteinuria was induced in male Wistar rats after a single intravenous injection of PAN (50 mg/kg) on Day 0. Treatment groups received pioglitazone (Pio, 10mg/kg; n = 7) or GQ-16 (40mg/kg; n = 7) daily by oral gavage for 11 days.

(A) Urinary protein/creatinine ratios (UPCr, Mean ± SEM) were plotted from Day 11 urine samples (*p<0.05, **p<0.01, ***p<0.001, ns= p>0.05; Mann-Whitney test).

(B) Representative gels showing urinary albumin bands after PAN injections and treatments with Pio and GQ-16. Equal volumes (5 μL) of urine from selected days were analyzed by SDS-polyacrylamide gel electrophoresis and Coomassie Blue staining.

(C) Serum albumin concentrations (Mean ± SEM) from Day 11 were plotted for the four groups (*p<0.05, ns = p>0.05; Mann-Whitney test).

(D) Linear regression was performed on all the rats combined which showed correlation of serum albumin with proteinuria.

(E–H) Histologic evaluation of kidneys stained with periodic acid-Schiff method (scale bar = 20 μm). PAN-injected rats (F) had dilated tubules that contained protein casts. These were not present in saline-injected rats (E) or in PAN injected rats that were treated with Pio (G) or GQ-16 (H). As expected in the model of minimal change disease, the glomeruli were normal.

transactivation assays (Figure S1)(Amato et al., 2012). It activated PPARγ in a dose-dependent manner and elicited ~30–50% of the maximal activity induced by the full agonist Pio (Figure S1). A single IV PAN injection of 50 mg/kg to male Wistar rats induced massive proteinuria on Day 11 (32.5 ± 9.3 mg/mg; p = 0.0006), which started appearing on Day 4 (Figures 2A and 2B). Control rats, which received IV saline injection, maintained baseline levels of urinary protein (2.3 ± 0.2 mg/mg). Daily Pio treatment resulted in a significant mean reduction in PAN-induced proteinuria to 64% (13.2 ± 5.5 mg/mg; p = 0.05). Interestingly, GQ-16 treatment decreased PAN-induced proteinuria more robustly to 81% reduction (8 ± 3.5 mg/mg; p = 0.004) (Figures 2A and 2B). In addition, the proteinuria levels with GQ-16 treatment were comparable to control levels, whereas Pio treatment remained significantly different from Control (p = 0.004).

Assessment of serum albumin levels in these rats showed a decrease in PAN injected rats as compared to control rats (2.2 ± 0.2 g/dL vs. 2.9 ± 0.2 g/dL; p = 0.02). Treatment with daily Pio resulted in a modest but insignificant increase in serum albumin (2.3 ± 0.1 g/dL; p = 0.26), whereas treatment with GQ-16 daily resulted in a significant increase in serum albumin levels (2.6 ± 0.1 g/dL; p = 0.014), which were comparable to control (p = 0.63, ns) (Figure 2C). In addition, serum albumin showed a significant correlation to proteinuria in all the rats combined (p = 0.02) (Figure 2D).

Histologic evaluation of kidneys from PAN rats revealed numerous dilated tubules with intratubular protein casts and minimal glomerular lesions as expected with the PAN model (Figures 2E and 2F). Some tubules were lined by

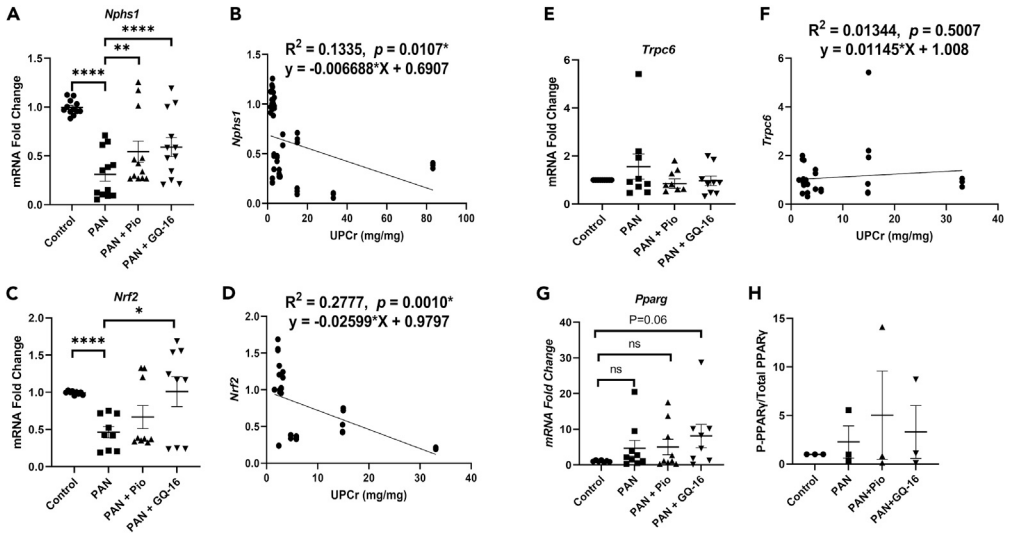

Figure 3. Glomerular gene expression of podocyte marker *Nphs1* and PPARγ target gene *Nrf2* is restored with treatment

Glomerular gene expression was measured by real time RT-PCR from total RNA extracted from the glomeruli isolated from Control, PAN-injected, and PAN-injected rats treated with Pio or GQ-16 (n ≥ 3/group, assay in triplicates).

(A, C, E, and G) Mean ± SEM plotted of (A) *Nphs1*, (C) *Nrf2*, (E) *Trpc6*, and (G) *Pparg*. (*p<0.05, **p<0.01, ***p<0.001, ****p<0.0001; Student's *t* test).

(B, D, and F) Gene expression was normalized to house-keeping gene *Rpl6*. Linear regression analyses were performed to correlate proteinuria with (B) *Nphs1*, (D) *Nrf2*, and (F) *Trpc6* expression.

(H) Phosphorylated-PPARγ at Serine 273 was measured and normalized to total PPARγ using total protein isolated from Control, PAN-injected, and PAN-injected rats treated with Pio and GQ-16 from glomeruli and plotted.

attenuated epithelium whereas others had hypertrophied epithelial cells, and there was mild multifocal lymphocytic inflammation. Tubular casts, tubular dilation, epithelial cell attenuation and hypertrophy and inflammation were all prevented by both Pio and GQ-16 treatments (Figures 2G and 2H), respectively.

Glomerular gene expression of podocyte marker *Nphs1* and PPARγ target gene *Nrf2* is restored with treatment with GQ-16

Because podocytopathy is a characteristic of proteinuria in glomerular disease and to understand the role of PPARγ activation in altering glomerular pathways, we measured the expression of relevant podocyte markers and genes in the glomeruli of nephrotic and treated rats. PAN-induced nephropathy resulted in a reduction in the glomerular expression of podocyte marker *Nphs1* (encoding for nephrin), a critical component of slit diaphragm, synpatopodin and *Nrf2* (encoding for nuclear factor erythroid 2-related factor 2), a target gene downstream of *PPARγ* (Figures 3A–3D and S2).*Nphs1* expression was down-regulated with PAN and significantly restored with GQ-16 treatment and modestly with Pio treatment (Figure 3A).*Nphs1* expression also correlated with reduction in proteinuria in these rats (p = 0.01) (Figure 3B). Notably, while GQ-16 treatment resulted in marked restoration of *Nrf2* expression, Pio treatment did not (Figure 3C), and *Nrf2* expression levels correlated strongly with reduction in proteinuria (p = 0.001) (Figure 3D). Although *Trpc6* (encoding for transient receptor potential cation channel, subfamily C, member 6) showed a trend toward induction with PAN and reduction with both Pio and GQ-16 treatments, its correlation with proteinuria was not found to be significant (Figures 3E and 3F). Furthermore, we found that our gene expression data corroborated the prediction of PPAR-responsive elements (PPREs) on the target genes measured in this study using the 'PPARgene' database (Table 1) (Fang et al., 2016). This database was developed using a machine learning method to predict novel PPAR target genes by integrating in silico PPRE analysis with high throughput gene expression data. For example, both *Nrf2* and *Nphs1* are predicted to contain PPREs flanking their transcription start sites.

Next, we determined the ability of Pio and GQ-16 to alter *Pparg* gene expression and its phosphorylation status at the Ser 273 position. PPARγ phosphorylation at Ser273 has been shown to be an important factor in determining activity for its insulin sensitizing effects (Choi et al., 2011; Hall et al., 2020), and thus to

Table 1. PPAR-responsive element (PPRE) prediction in target genes

Gene	Tissue (Current Study)	p Value[a]	Confidence Level	PPREs Predicted[b]
Nrf2	Glomerular	0.45663	Low	7
Nphs1	Glomerular	0.63696	Medium	4
Trpc6	Glomerular	–	–	–
Ap2/Fabp4	WAT	0.99997	High	10
Cd36	WAT	0.97886	High	3
Adipoq	WAT	0.97153	High	12
Pparg	Glomerular/WAT	0.91081	High	2
Pgc1a	WAT	–	–	–
Adipsin	WAT	0.96216	High	6
Albumin	Hepatic	0.63443	Medium	2
Abca1	Hepatic	0.99483	High	3
Pcsk9	Hepatic	–	–	–
F2	Hepatic	0.55991	Low	4
Serpinc1	Hepatic	–	–	–
Ppia	Housekeeping (WAT, hepatic)	–	–	–
Rpl6	Housekeeping (glomerular)	–	–	–

[a]Probability of being a PPAR target gene, higher value means a higher confidence. High-confidence ($p > 0.8$), median-confidence ($0.8 \geq p > 0.6$), low-confidence category ($0.6 \geq p > 0.45$).Genes with p value ≤ 0.45 were predicted as negative.
[b]Putative PPREs in the 5Kb transcription start site (TSS) flanking region.

understand its role in the reduction of proteinuria, we measured its levels in the glomeruli of nephrotic and Pio and GQ-16- treated rats. Although *Pparg* expression tended to be greater in PAN and PAN + Pio groups compared to control, and somewhat increased with GQ-16 treatment, it was not significant ($p = 0.06$) (Figure 3G) and the overall expression in all the rats did not correlate with proteinuria (data not shown). Furthermore, the phosphorylation status of PPARγ at Ser273 position was unaltered with Pio and GQ-16 in PAN-nephrotic rats (Figures S3 and 3H), and it did not correlate with proteinuria.

RNASeq analysis reveals that Pio and GQ-16 restore common and distinct glomerular genes, pathways, and downstream processes

Injury with PAN resulted in 1089 DE-Gs compared to controls, and 26 of these DE-Gs were restored by both Pio and GQ-16 treatments, whereas 106 unique GQ-16 regulated DE-Gs and 17 unique Pio-regulated DE-Gs were identified (Figure 4A). Overall, Pio and GQ-16 treatment resulted in 75 and 173 DE-Gs compared to PAN injury, which included 29 common and 190 distinct genes (Figure 4A). Of the 29 common DE-Gs, 28 DE-Gs were down-regulated by both Pio and GQ-16 and only 1 DEG upregulated by both treatments when compared to PAN (Figure 4B). Of the 190 distinct DE-Gs identified between Pio and GQ-16 treatments, 41 were down-regulated and 5 up-regulated by Pio and 124 down-regulated and 20 up-regulated by GQ-16 treatment. Figure 4C depicts a heatmap of all the DE-Gs between PAN versus Control and those restored by (1) only GQ-16, or (2) both or (3) only Pio treatments. IPA of DE-Gs between PAN+Pio vs. PAN (75 DE-Gs) and PAN + GQ-16 vs. PAN (173 DE-Gs) revealed the top canonical glomerular pathways that are associated with the proteinuria reducing beneficial effects of Pio and GQ-16, respectively (Figures 4D and 4E). These include the IL-8, IL-12 and NF-κB pathways for Pio and cell cycle regulation and matrix metalloprotease pathways for GQ-16. Furthermore, ontology enrichment analysis identified the top biological processes (Figures S4 and S5), cellular components (Figures S6 and S7) and molecular functions (Figures S8 and S9) associated with each treatment.

Glomerular disease associated hypercoagulopathy is corrected with GQ-16 treatment

We have previously shown a significant correlation between hypercoagulopathy and proteinuria during NS, and correction of hypercoagulopathy with glucocorticoid treatment, which is a standard treatment for NS (Kerlin et al., 2015; Waller et al., 2020). We thus measured thrombin generation parameters in our model of

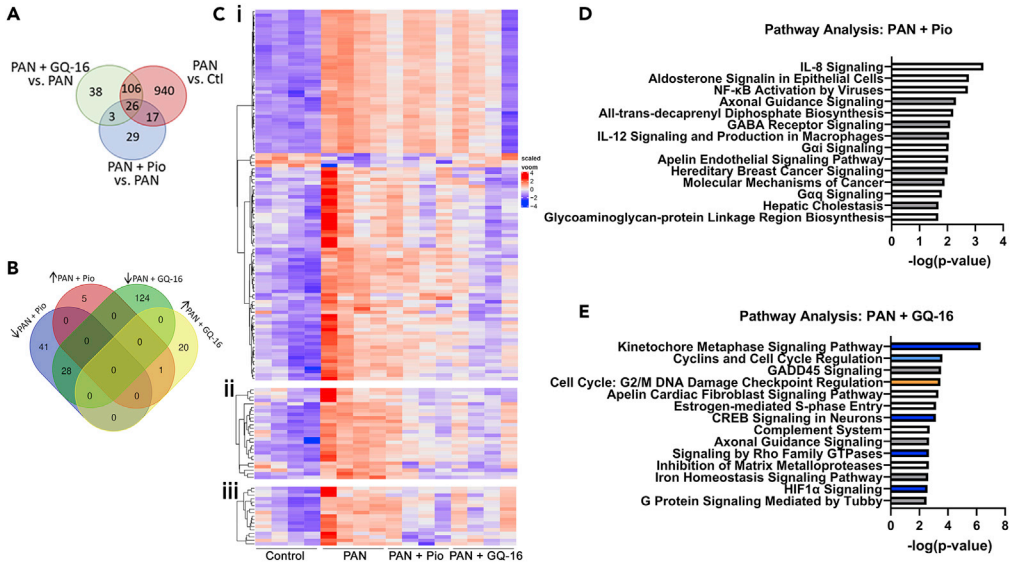

Figure 4. RNASeq analysis reveals that Pio and GQ-16 restore common and distinct glomerular genes, pathways and downstream processes

(A) Differentially expressed genes (DE-Gs) between PAN vs. Control (pink circle-1089), PAN + GQ-16 vs. PAN (green circle-173) and PAN + Pio vs. PAN (blue circle-75) are depicted (N = 4/group, $p<0.05$). Venn diagrams highlight the number of genes that are commonly (26 DE-Gs between all 3 groups) or distinctly regulated by the 3 groups (PAN, PAN + Pio and PAN + GQ-16).

(B) Venn diagram highlights the DE-Gs that are up- or down-regulated with Pio and GQ-16 and those that are common and distinct between the two treatment groups, compared to PAN injury.

(C) Heatmap of DE-Gs between PAN vs. Control and those restored by (i) only GQ-16, or (ii) both or (iii) only Pio, treatments.

(D and E) Top predicted enriched pathways from Ingenuity Pathway Analysis (IPA) of DE-Gs between (D) PAN + Pio vs. PAN (75 DE-Gs) and (E) PAN vs PAN + GQ-16 vs. PAN (173), are listed and those with positive z-score are denoted in orange, negative z-score in blue, and z score = 0 in white.

NS, their alteration with treatment with Pio and GQ-16, and correlation with proteinuria. A typical thrombin generation curve, as shown in Figure 5A, is characterized by a short lag phase, the area under the curve (endogenous thrombin potential), peak thrombin, and velocity index (Castoldi and Rosing, 2011). Representative curves from each of the study groups are shown in Figure 5B. Endogenous thrombin potential (ETP) is a consistently elevated thrombin generation parameter in NS (Kerlin et al., 2015; Waller et al., 2020), and we found it to be significantly increased in nephrotic rats (PAN, 3646 ± 199 nM*min vs. Control, 2445 ± 402 nM*min; $p = 0.014$) (Figures 5B and 5C). This increase in ETP with PAN showed significant reduction with GQ-16 treatment (2544 ± 489 nM*min; $p = 0.049$), while Pio treatment did not have a detectable effect (3509 ± 428 nM*min; $p = 0.77$) (Figures 5B and 5C). Notably, ETP strongly correlated with proteinuria ($p = 0.01$) in the nephrotic and treatment rats combined (Figure 5D). In addition to ETP, other parameters such as peak thrombin generation, lag phase, and velocity index were also derived from these thrombin generation assays (Table 2). The time of the lag phase was significantly reduced with PAN compared to Control, and it showed a tendency to reverse back toward Control with GQ-16 treatment (Table 2).

GQ-16 treatment reduces glomerular disease-associated hypercholesterolemia and alters hepatic gene expression

Dyslipidemia is a major feature of NS and glomerular disease (Agrawal et al., 2018), manifesting as hypercholesterolemia. To understand the role of PPARγ agonists in altering dyslipidemia and the expression of genes involved in lipid metabolism, we measured total cholesterol levels in the serum and the expression of relevant genes in the liver of nephrotic and treated rats. PAN-induced nephropathy resulted in significant increase in total cholesterol levels compared to control (PAN, 161.6 ± 37.6 mg/dL vs. Control, 81.7 ± 2.7; $p = 0.006$) (Figure 6A). GQ-16 and Pio treatments resulted in significant mean reduction of PAN-induced hypercholesterolemia to 86% (93.1 ± 13.4 mg/dL; $p = 0.019$) and 80% (97.9 ± 12.4 mg/dL; $p = 0.01$),

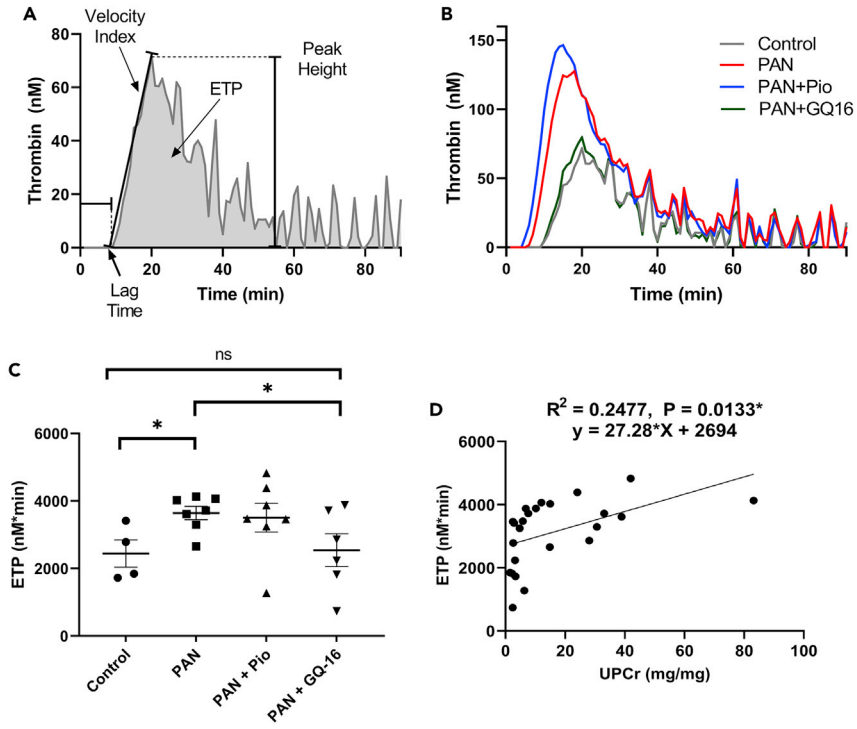

Figure 5. Glomerular disease associated hypercoagulopathy is corrected with GQ-16 treatment

Endogenous thrombin potential (ETP) was measured using a thrombin generation assay (TGA) on plasma from rats in each group of PAN-injured, and Pio and GQ-16 treated rats (n = 4–7/group).

(A) Typical thrombin generation curve with ETP, peak height, velocity index, and lag time are labeled.

(B) Representative graphs of thrombin generation from one rat from each group.

(C) Mean ± SEM of ETP plotted with the individual values shown.

(D) Linear regression analysis to correlate proteinuria with ETP. Student's ttest.*p<0.05.

respectively. Moreover, serum cholesterol levels strongly correlated with proteinuria ($p < 0.0001$) in the nephrotic and treatment rats combined (Figure 6B). *Pcsk9* (encoding for proprotein convertase subtilisin/kexin type 9) expression in the liver tissue was significantly upregulated with PAN-induced nephropathy (~30-fold) and restored to control levels with both GQ-16 and Pio treatments (Figure 6C). Although *Abca1* (encoding for ATP binding cassette subfamily A member 1) expression was unchanged with PAN, it was increased ~23-fold with GQ-16 treatment (Figure 6D).

As liver is also the primary source of albumin (*Alb*) and coagulation proteins, such as prothrombin (*F2*) and antithrombin (*SerpinC1*), and we have observed hypoalbuminemia and hypercoagulopathy with PAN injury and their respective corrections with GQ-16, we measured the hepatic gene expression in the nephrotic and treatment rats (Figure S10). Although *Alb* was not induced with PAN, both *F2* and *SerpinC1* showed a tendency to be induced with PAN and reduced with GQ-16 ($p = 0.07$).

GQ-16 and Pio treatments distinctly alter adipogenesis and gene expression of adipogenic pathways

Adipogenesis and adipogenic pathways are typically induced with PPARγ activation and we thus measured alterations in lipid accumulation and the expression of genes involved in these pathways in differentiated adipocytes *in vitro* and in the epididymal fat of WAT *in vivo* with Pio and GQ-16 treatments. Although both Pio and GQ-16 induced lipid accumulation in differentiated adipocytes in a dose-dependent manner, Pio induced significantly much higher lipid accumulation compared to GQ-16 (Figure 7Ai and ii). In accordance, expression of *Ap2* (*Fabp4*, encoding for fatty acid binding protein 4), which causes weight gain, was more pronounced and significant with Pio as compared to GQ-16 in both differentiated adipocytes (Figure 7Aiii) as well as in WAT (Figure 7Bi). On the other hand, expression of insulin sensitizing or secreting adipokines, *Adipoq* (adiponectin) and *Adipisn* (*Cfd*, complement factor D) was induced more robustly with

Table 2. Coagulation and thrombin generation parameters

Parameters	Control	PAN	PAN + Pio	PAN + GQ-16	UPCr Correlation R^2	UPCr Correlation p value
ETP (nM*min)	2445 ± 402.1	3646 ± 198.8* (p = 0.0143)	3509 ± 427.8	2544 ± 489.0# (p = 0.0493)	0.2477	0.0133±
Peak Thrombin (nM)	98.97 ± 20.82	180.4 ± 27.02 (p = 0.0698)	180.8 ± 29.50	134.0 ± 35.54	0.0282	0.4328
Velocity Index (nM/min)	16.08 ± 5.073	33.07 ± 8.570	34.67 ± 8.448	19.91 ± 6.643	0.0037	0.7775
Lag Phase (min)	10.38 ± 0.826	6.321 ± 0.713** (p = 0.006)	7.714 ± 0.6974	9.250 ± 1.532 (p = 0.0956)	0.2035	0.0269±

*p < 0.05; compared to Control.
**p < 0.01; compared to Control.
#p < 0.05; compared to PAN.
±p < 0.05; correlation.

GQ-16 as compared to Pio (Figure 7B ii and iii). Although a trend was observed toward an increase in *Cd36* (fatty acid transporter) expression, with both Pio and GQ-16, no significant differences were observed (Figure S11). Notably, as opposed to the studies involving PPARγ in the context of diabetes and obesity, it is not feasible to study the direct effect of weight gain in the current study as PAN-induced treatment itself leads to a modest reduction in weight gain in these rats and limited duration of the study. Nevertheless, we observed that while the weight reduction in nephrotic rats was maintained with GQ-16 treatment, Pio treatment did not show any significant difference from control rats (Figure S12).

GQ-16 treatment induces *Pparg* expression and reduces Δexon-5 splice variant form

Although PPARγ co-activator 1α (*Pgc1α*) showed a trend in increase with Pio and GQ-16 treatments (Figure 8A), both treatments induced the expression of *Pparg* (Figure 8B), which seemed to be more prominent in WAT than in the glomeruli (Figures 8B and 3G). In addition, recently, a naturally spliced variant form of *PPARG* has been identified in human adipocyte progenitor cells and in WAT of obese and diabetic patients (Aprile et al., 2018). We were able to detect the expression of a Δ exon 5 splice variant form of *Pparg*, which was found to be decreased with injury as well as with both Pio and GQ-16 treatments in the WAT when normalized to the total *Pparg* expression (Figure 8C). Notably, GQ-16 further reduced the levels of Δexon 5 *Pparg* variant.

DISCUSSION

Glomerular disease is the leading cause of ESKD in the US, and NS, characterized by high-grade proteinuria, is one of the most common forms of glomerular disease (Floege et al., 2019; Luyckx et al., 2018; Rovin et al., 2019). Furthermore, NS is typically associated with hypoalbuminemia, hypercholesterolemia, systemic immune dysregulation, hypercoagulopathy, and edema (Agrawal et al., 2018; Araya et al., 2006, 2009; Radhakrishnan, 2020; Siddall and Radhakrishnan, 2012). Standard treatments include glucocorticoids (for idiopathic and primarily pediatric NS), but their use leads to side effects, and 10–50% of adult and pediatric NS patients can be resistant to steroid treatment (Canetta and Radhakrishnan, 2015; Eddy and Symons, 2003; Nourbakhsh and Mak, 2017). Some NS patients exhibit hypertension, which can be managed with ACE inhibitors and ARBs, while reducing proteinuria. Moreover, steroid-resistant NS is associated with an increased risk of developing CKD, which account for 15% of all children with CKD requiring renal replacement therapy (Weaver et al., 2017). Thus, there is an urgent and critical need to develop new alternative therapies for NS and glomerular disease with increased efficacy and reduced side effects. In order to do so, we and others have previously reported that PPARγ agonists not only provide beneficial protective effects in type II diabetes and DN, but also in various models of non-diabetic glomerular disease (Agrawal et al., 2016, 2021; Henique et al., 2016; Ma et al., 2001; Platt and Coward, 2016; Sonneveld et al., 2017; Yang et al., 2006, 2009; Zuo et al., 2012). However, targeting PPARγ via widely marketed anti-diabetic drugs (traditional TZDs) has been re-evaluated because of significant side effects such as adipogenic weight gain, heart failure, bone fracture, and bladder cancer (Friedland et al., 2012; Nesto et al., 2003; Nissen and Wolski, 2007; Tang et al., 2018; Viscoli et al., 2017; Yki-Jarvinen, 2004). In the current study,

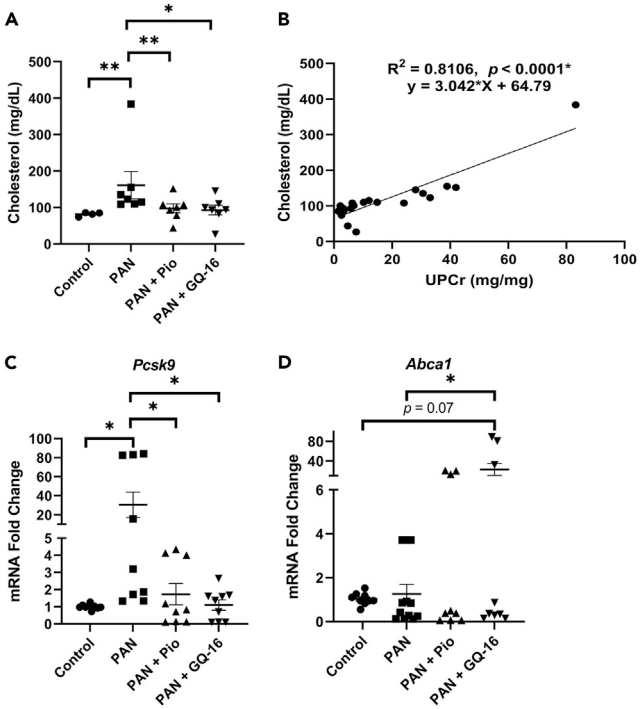

Figure 6. GQ-16 treatment reduces glomerular disease-associated hypercholesterolemia and alters the hepatic gene expression

(A) Serum cholesterol concentration was measured from Day 11 serum samples and (A) plotted as Mean ± SEM.

(B) Linear regression correlating serum cholesterol with proteinuria. Hepatic gene expression was measured by real time RT-PCR from total RNA extracted from liver tissue from Control, PAN-injected, and PAN-injected rats treated with Pio and GQ-16 (n ≥ 3/group, assay in triplicates).

(C) *Pcsk9* and (D) *Abca1* gene expression was normalized to liver housekeeping gene *Ppia*. Mean ± SEM plotted; Student's ttest. *p<0.05, **p<0.01.

we demonstrate that unlike the full agonist of PPARγ Pio, a selective partial agonist GQ-16 can mechanistically dissociate the downstream effects of PPARγ to efficaciously reduce proteinuria in a PAN-induced animal model of glomerular disease/NS (Figure 9, Table 3). Although GQ-16 mirrored some of the effects of Pio such that it restored glomerular *Nphs1* and hepatic *Pcsk9* expression and reduced hypercholesterolemia, the selective beneficial effects of GQ-16 were also associated with restoration of glomerular *Nrf2*, and reduction in other disease-associated co-morbidities i.e., hypoalbuminemia and hypercoagulopathy. Furthermore, our findings strengthened the notion that compared to Pio, GQ-16 treatment caused less lipid accumulation in differentiated adipocytes and did not cause induction of *Ap2* (fatty acid binding protein) both in adipocytes and WAT, which are factors attributed to the limitations of Pio use in patients. Taken together, these findings suggest that PPARγ can be differentially modulated by its partial agonist GQ-16, to impart the desired proteinuria-reducing effects with reduced NS associated co-morbidities, while reducing the side effects conferred by traditional PPARγ full agonists.

PPARγ is attributed to the therapeutic basis of TZDs to treat diabetes because it improves insulin sensitivity and decreases insulin demands (Yki-Jarvinen, 2004). Although PPARγ is the master regulator of glucose and lipid metabolism and regulator of adipogenesis, pre-clinical studies and meta-analyses have now highlighted its direct beneficial role in kidney cells in addition to its favorable systemic effects in the context of diabetes (Buckingham et al., 1998; Tanimoto et al., 2004). Notably, in the last decade, we and others have documented the beneficial roles of TZDs in directly protecting podocytes from injury (Agrawal et al., 2011; Kanjanabuch et al., 2007; Miglio et al., 2011, 2012), in reducing proteinuria and glomerular injury in various animal models of glomerular disease such as minimal change disease, focal segmental glomerulosclerosis (FSGS), and crescentic glomerulonephritis(Agrawal et al., 2016; Henique et al., 2016; Ma et al., 2001; Platt and Coward, 2016; Sonneveld et al., 2017; Yang et al., 2006, 2009; Zuo et al., 2012), and in improving clinical outcomes in NS patients refractory to steroid treatment (Agrawal et al., 2016; Hunley et al., 2019). More

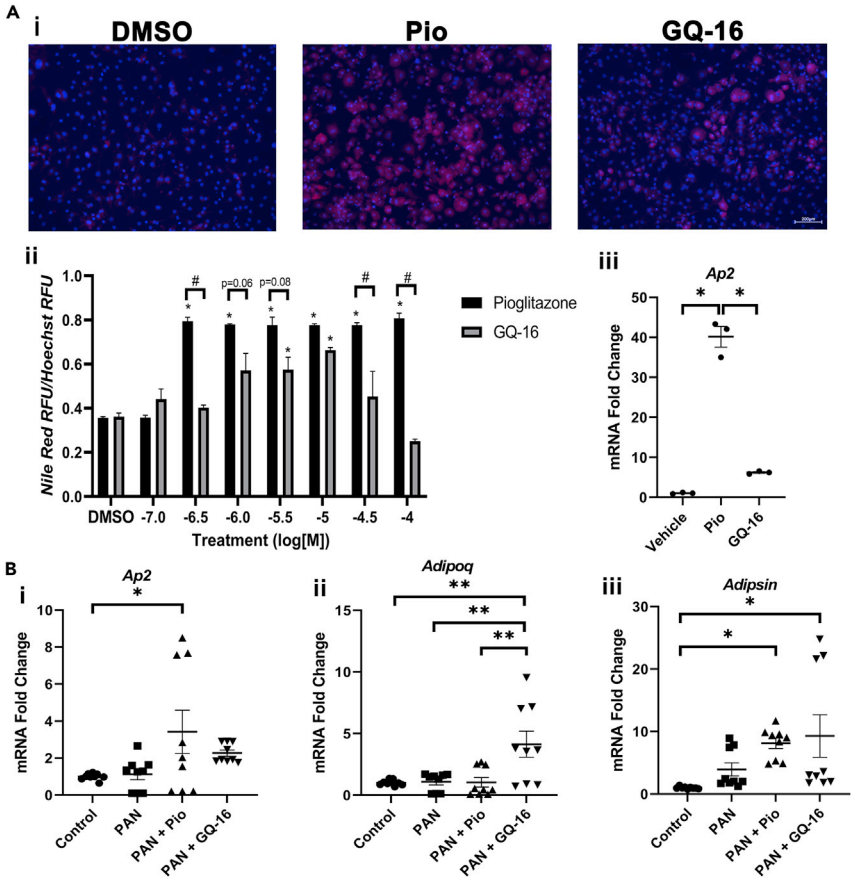

Figure 7. GQ-16 and Pio treatments distinctly alter adipogenesis and gene expression of adipogenic pathways

(A) 3T3-L1 preadipocytes were cultured and differentiated and assessed for (1) lipid accumulation by fluorescence microscopy to visualize intracellular lipids stained with Nile Red and nucleic acid stained with Hoechst 33342 (scale bar = 200 μm), (2) quantitative lipid accumulation by measuring and plotting relative fluorescence units (RFU) (*$p < 0.05$ vs DMSO, #$p < 0.001$; one-way ANOVA), and (3) gene expression of *AP2/FABP4*, in response to Pio and GQ-16 treatments (*$p < 0.05$; one-way ANOVA). Mean ± SEM plotted and each experiment was performed at least in triplicate.

(B) White adipose tissue gene expression was measured by real time RT-PCR from total RNA extracted from epididymal fat tissue from Control, PAN-injected, and PAN-injected rats treated with Pio and GQ-16 ($n \geq 3$/group, assay in triplicates). Expression of mRNA from (i)*Ap2*, (ii)*Adipoq*, and (iii)*Adipsin* was determined and normalized to the fat housekeeping gene *Ppia*. Mean ± SEM plotted, one-way ANOVA; *p<0.05, **p<0.01, ***p<0.001, ****p<0.0001.

recent discoveries suggest that the beneficial insulin-sensitizing activities of PPARγ can be dissociated from its harmful adipogenic activities (Choi et al., 2010,2011;Haberman Associates, 2010, 2011; Hall et al., 2020). This has led to the development of mechanistically distinct novel compounds, such as MRL24, SR1664 and GQ-16. MRL24 and SR1664 have been demonstrated to inhibit CDK5-mediated phosphorylation of PPARγ at its Ser273 position (like TZDs) to provide anti-diabetic effects while dissociating its classical receptor transcriptional agonism (unlike traditional TZDs) (Choi et al., 2010, 2011). GQ-16 was specifically developed because of its distinct binding profile to PPARγ compared to traditional TZDs and it has been shown to have weak traditional PPARγ agonistic activity (adipogenic) and associated weight gain effects, but very good anti-diabetic activity (Amato et al., 2012; Coelho et al., 2016).

The current study uncovers the proteinuria reducing effects of GQ-16 in a rat model of NS. The 84% reduction in proteinuria by GQ-16 compared to PAN-nephrosis was almost comparable to controls as well as to the previously described reduction with high dose glucocorticoids (79%) in this model (Agrawal et al., 2016). GQ-16 treatment was also effective in correcting hypoalbuminemia in PAN NS. Several possible mechanisms can be attributed to these observed beneficial effects of GQ-16. Podocyte injury and loss are characteristic features of proteinuria in NS, and Nephrin (*Nphs1*), an essential component of the podocyte slit diaphragm, plays an important role in podocyte integrity which is compromised in

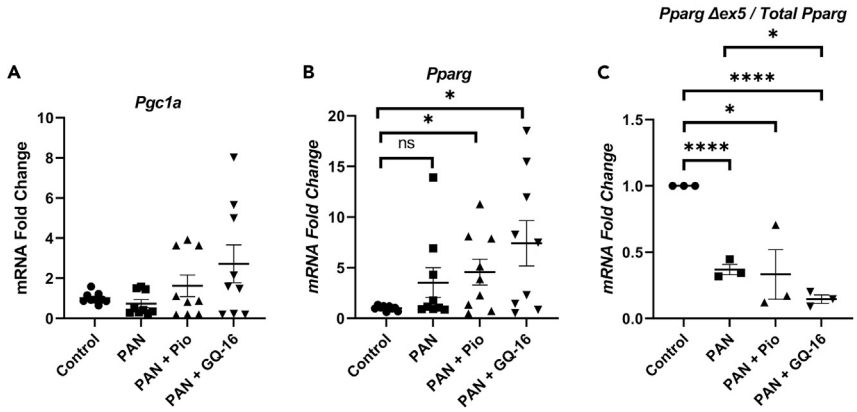

Figure 8. GQ-16 Treatment induces *Pparg*expression and reduces Δexon-5 splice variant form

White adipose tissue gene expression was measured by real time RT-PCR from total RNA extracted from epididymal fat tissue from Control, PAN-injected, and PAN-injected rats treated with Pio and GQ-16 (n ≥ 3/group, assay in triplicates). (A and B) Expression of mRNA from (A) *Pgc1a*, and (B) *Pparg* was determined and normalized to the fat house-keeping gene *Ppia*.

(C) Expression of *Pparg*Δ exon 5 splice variant form was measured and normalized to *Pparg*. Mean ± SEM Student's *t*test. *p<0.05, **p<0.01, ***p<0.001, ****p<0.0001.

proteinuria and nephrosis (Agrawal et al., 2016; Grahammer et al., 2013; Kestila et al., 1998; Khoshnoodi et al., 2003). We found that *Nphs1* expression inversely correlated with proteinuria and it was significantly restored with GQ-16 treatment. Remarkably, the decrease in the expression of master regulator of oxidation pathways, *Nrf2* within the glomeruli of nephrotic rats was largely restored with only GQ-16, but not by Pio. The latter may explain the putative cytoprotective and anti-inflammatory effects imparted by GQ-16 in the nephrotic rat model. It is also likely that the restoration of NRF2 may have played a role in regulating PPARγ expression (Lee, 2017) to reduce the severity of the course of glomerular disease (Henique et al., 2016). PPARγ has been shown to be phosphorylated in obesity models at the Ser273 site and dephosphorylated with the insulin sensitizing effects of PPARγ agonists (Choi et al., 2010, 2011; Hall et al., 2020). In an *in vitro* assay, GQ-16 has been shown to dephosphorylate PPARγ like traditional TZDs (Amato et al., 2012; Coelho et al., 2016). Interestingly, our results demonstrated that relative phosphorylated PPARγ levels (at Ser273) remain unaltered with PAN injury and subsequent Pio and GQ-16 treatments. This suggests that while PPARγ-Ser273 is known to play a major role in determining the insulin sensitizing effects of PPARγ in adipose tissue, the same mechanism may not play a role in determining its proteinuria-reducing effects in glomeruli. Likewise, our data failed to support the involvement of TRPC6 involvement that was reported to increase with glomerular injury and proteinuria as we did not observe any changes during PAN nephrosis with a decrease in its expression in the presence of either PPARγ agonists. Finally, global analysis of glomerular transcriptome data supported that the observed effects of Pio and GQ-16 treatments are likely associated with elicitation of both common and distinct glomerular DE-Gs, pathways and biological processes. Collectively, we interpret our findings as GQ-16 is perhaps more efficacious than Pio or at least equally as Pio in reducing glomerular injury and proteinuria.

The current study also studies the beneficial effect of GQ-16 on NS associated co-morbidities such as hypercoagulopathy and dyslipidemia, which are likely independent of its glomerular effects. Our previous observations have found increased ETP (an excellent measure of hypercoagulopathy) to be very well-correlated with increased proteinuria in NS and its decrease with standard treatment in both human studies and in animal models (Kerlin et al., 2015; Waller et al., 2020). Interestingly, in the current study, we found a good correlation of ETP with proteinuria, significant increase with injury, and a significant decrease with GQ-16 treatment only. An earlier study from our group demonstrated that whereas Pio decreased ETP (measured after a longer stretch of time post-Pio dosage compared to this study) in concert with proteinuria, it significantly increased ETP when given to healthy control rats, suggesting its inherent role in increasing ETP (Waller et al., 2020). In addition, dysregulated lipid metabolism is one of the other major features of NS and glomerular disease (Agrawal et al., 2018). Hepatic levels of PCSK9 are known to be upregulated in glomerular disease which contributes to dyslipidemia by degrading the low-density lipoprotein (LDL) receptor and decreased LDL uptake by the liver (Agrawal et al., 2018). Inhibition of PCSK9 using anti-PCSK9

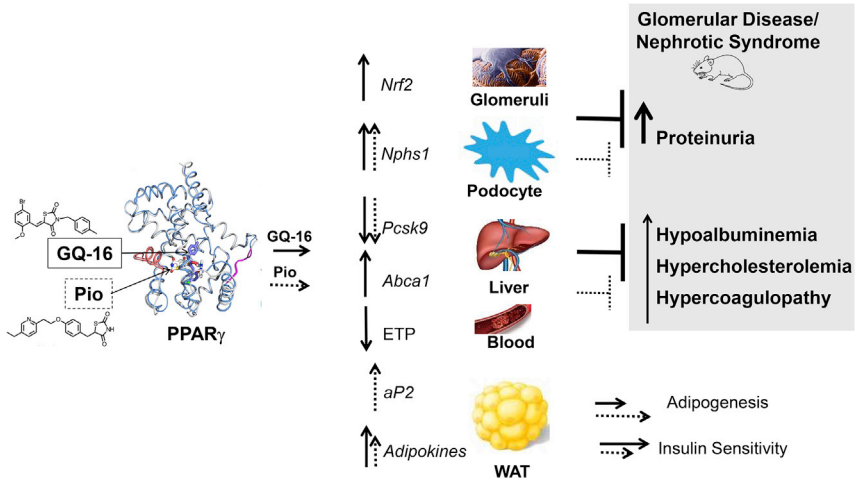

Figure 9. Schematic depicting the beneficial effects of GQ-16 in improving glomerular disease

The traditional full agonist of PPARγ, pioglitazone (Pio) and the partial agonist and selective modulator, GQ-16, both bind and activate PPARγ, although in distinct ways. While GQ-16 activates PPARγ differently than Pio, it is equally or more efficacious in reducing proteinuria and overall nephrotic syndrome-associated co-morbidities such as hypoalbuminemia, hypercholesterolemia and hypercoagulopathy (see Table 3). These effects are associated with increased glomerular *Nrf2* expression, increased expression of *Nphs1* in podocytes, decreased hepatic expression of *Pcsk9* and increased hepatic *Abca1* expression, and reduced endogenous thrombin potential (ETP) in the plasma of nephrotic rats treated with GQ-16. Moreover, GQ-16 induces adipocyte lipid accumulation and white adipose tissue (WAT) *aP2* to a lesser extent than Pio and it increases the expression of adipokines to a larger extent than Pio, which likely renders reduced adipogenesis and increased insulin sensitivity as compared to Pio (see Table 3). Solid arrows and lines represent GQ-16 effects and dashed arrows and lines represent the effects of Pio.

monoclonal antibodies and siRNAs has gained high clinical importance because of its lipid-lowering effects in the conditions of hypercholesterolemia and is now gaining traction in the context of NS (Agrawal et al., 2018; Awanami et al., 2017; Di Bartolo et al., 2017; Fitzgerald et al., 2017; Morris, 2016). Our results corroborate the importance of PCSK9, as we found a significant induction in its gene expression in the liver of nephrotic rats and reduction with both Pio and GQ-16 treatments. The effects of other players such as ABCA1 were variable although we observed a significant increase in its expression with GQ-16 treatment, but only a trend with Pio in our animal model of NS. Overall, our findings identify reduction of NS-induced hypercholesterolemia with GQ-16, in agreement with the previously observed effects of GQ-16 in reducing high-fat diet-induced hepatic triglyceride content and steatosis (Coelho et al., 2016).

GQ-16 exhibits lower adipogenic activity when compared to TZDs as shown by reduced transactivation activity and *Ap2* induction (Amato et al., 2012; Coelho et al., 2016). Findings in obese Swiss male mice indicated that in addition to exhibiting insulin-sensitizing properties, 14-day treatment with GQ-16 induced decreased edema, weight gain, and visceral WAT mass in response to high fat diet, despite increasing energy consumption (Amato et al., 2012; Coelho et al., 2016). These effects were accompanied by the induction of thermogenesis-related genes in epididymal fat depots, suggesting that browning of visceral WAT may have contributed to weight loss. These results strongly support that PPARγ activation by partial agonists, devoid of full agonism-related unfavorable effects, may be a strategy to induce browning of WAT and hence to treat obesity and diabetes. Specifically, our current study supports this theory in the context of non-diabetic disease. Our studies indicate that Pio induces increased lipid accumulation and *Ap2* induction as compared to GQ-16 in differentiated adipocytes. Similar induction of *Ap2* was also observed in the WAT of Pio-, but not GQ-16, treated rats. Furthermore, both full and partial PPARγ agonists are known to increase the expression of insulin sensitizing adipokines, adiponectin, and adipsin, as well as the fatty acid transporter CD36 (Choi et al., 2010). We observed that both Pio and GQ-16, induced *Adipsin* and *Adipoq* expression, and overall, our results suggest that GQ-16 has a lower adipogenic profile than Pio, which would potentially offer a therapeutic advantage during long term treatment.

PPARγ exists in mainly two major isoforms, γ1 and γ2, which are a result of different promoter usage as well as alternative splicing (Figure 1) (Agrawal et al., 2021; Fajas et al., 1997; Mukherjee et al., 1997). Although γ1

Table 3. Summary of the beneficial and adverse effects of pioglitazone and GQ-16

NS Parameters	Control	PAN	PAN + Pio	PAN + GQ-16
Proteinuria	0%	100%	64%*	81%**
Co-morbidities				
Hypercoagulopathy	0%	100%	11%	92%*
Hypercholesterolemia	0%	100%	80%**	86%*
Hypoalbuminemia	100%	0%	25%	69%$
TZD Parameters		Vehicle Control	Pio	GQ-16
Adipogenesis				
aP2 (adipocytes)		100%	242 %#	127%
aP2 (WAT)		100%	3,815 %#	504%
Adipokines				
Adiponectin (WAT)		100%	3%	310%##
Adipsin (WAT)		100%	712%#	829%#

*p<0.05.
**p<0.01; reduction compared to PAN.
$p<0.05; increase compared to PAN.
#p<0.05.
##p<0.01; increase compared to Vehicle Control.

is ubiquitously expressed, including in podocytes, γ2 is mostly restricted to adipose tissue and liver (data not shown). Moreover, the recently identified Δ exon-5 splice variant form of *Pparg* in the adipose tissue has been shown to positively correlate with body mass index in obese and diabetic patients and function as a dominant negative form by reducing the adipogenic potential of precursor cells (Aprile et al., 2018). We have observed the presence of a Δ exon5 spliced form of *Pparg* in the WAT, which was reduced with PAN injury and further decreased with GQ-16 treatment. We speculate that any decrease in Δexon5 *Pparg* with PAN injury could likely be an adaptive mechanism, and its further reduction by GQ-16 could serve as a positive feedback loop to enhance PPARγ activity. Moreover, we were able to only detect a very minimal expression of this variant in human podocytes and none in the rat glomeruli, suggesting that this variant form probably does not play a major role in these cells/tissues.

Conclusions

In summary, our studies suggest that selective modulation of PPARγ by a partial agonist is efficacious in reducing proteinuria and is perhaps more beneficial than a full PPARγ agonist in reducing hypoalbuminemia and hypercoagulopathy, while providing reduced adipogenic potential and drug-induced side effects in a PAN-induced model of NS. Our findings not only emphasize the benefits of GQ-16 as a novel therapeutic modality for NS and deepen our molecular understanding of the role of PPARγ in glomerular disease but open new possibilities and potential future clinical implications for selectively modulating PPARγ by partial agonists for the treatment of glomerular disease. In this regard, designing novel modulators of PPARγ which would result in its optimal conformation that would yield desirable molecular and clinical effects would be highly significant.

Limitations of the study

Although we have demonstrated the efficacious and beneficial role of GQ-16 in PAN-nephrosis, future studies in other non-diabetic models of glomerular disease, such as chronic PAN, FSGS, or even immune-mediated forms of glomerular disease could examine a broader treatment potential for GQ-16. Moreover, future research examining the effects after disease onset could enhance the clinical appeal of the beneficial effects of GQ-16. Nevertheless, our study provides a proof of concept for protection of experimental NS with a selective PPARγ modulator and opens new avenues of designing or adapting new modulators of PPARγ for the treatment of glomerular disease. Further, whereas we have measured dose-dependent effects and drawn comparisons of GQ-16 and Pio in PPARγ activation, lipid accumulation, and *Ap2* induction, and demonstrated decreased PPARγ activation with a lower adipogenic profile of GQ-16 compared to Pio, our *in vivo* studies are limited by a single dose study. However, we have scaled the *in vivo* doses for the two compounds, based on the *in vitro* results and previous *in vivo* studies in which

we observed protective effects of Pio in NS (Agrawal et al., 2016) and reduced adipogenic profile of GQ-16 (Coelho et al., 2016). Although it is not feasible to study weight gain in a short-term nephrosis model, a real clinical scenario would benefit from long term treatment with a compound which offers reduced weight gain potential. The major strength of our study is that GQ-16 has equal or higher efficacious proteinuria-reducing effects than Pio, reduction in NS-associated co-morbidities while providing reduced adipogenic effects, as measured by reduced *Ap2* induction *in vitro* and *in vivo* and lipid accumulation *in vitro* as compared to Pio.

STAR★METHODS

Detailed methods are provided in the online version of this paper and include the following:

- KEY RESOURCES TABLE
- RESOURCE AVAILABILITY
  - Lead contact
  - Materials availability
  - Data and code availability
- EXPERIMENTAL MODELS AND SUBJECT DETAILS
  - Animals
  - Cell cultures
- METHOD DETAILS
  - Urinalysis
  - Serum chemistry
  - Coagulopathy measurement
  - RNA isolation, qRT-PCR
  - RNA seq, pathway analysis and ontology enrichment
  - Protein isolation, SDS-PAGE and western blotting
  - Immunofluorescence staining
  - PPARγ activation luciferase assay
  - Lipid accumulation assessment and *aP2* induction
  - Lipid accumulation assessment
  - *aP2* induction
  - PPAR-responsive element prediction
- QUANTIFICATION AND STATISTICAL ANALYSIS

SUPPLEMENTAL INFORMATION

Supplemental information can be found online at https://doi.org/10.1016/j.isci.2022.104001.

ACKNOWLEDGMENTS

We thank Jeffrey Miner, Washington University, St Louis, Missouri for his valuable comments and suggestions and for his mentorship on the American Heart Association Career Development Award granted to SA. We also thank Alexander S Banks, Beth Israel Deaconess Medical Center, Harvard Medical School, Boston, MA for critical comments and review of the manuscript. We thank the Genomics Core Resources at The Ohio State University for RNA Sequencing Services. This study was supported by the American Heart Association Career Development Award (CDA34110287) and funds from Nationwide Children's Hospital, United States to SA. The project described was also funded by the Center for Clinical and Translational Science Genomics Shared Resource Voucher Support to SA which was supported by the NIH Clinical and Translational Science Award to The Ohio State University (Award Number UL1TR002733) from the National Center for Advancing Translational Sciences, United States.

AUTHOR CONTRIBUTIONS

CB performed experiments, analyzed and interpreted the data, prepared figures and tables, and drafted the manuscript. GR, APW, and AAA performed experiments and edited the manuscript. BAK and APW interpreted the coagulopathy data and edited the manuscript. RC performed the histological analysis and edited the manuscript. MRG synthesized and provided the compound GQ-16 for these studies and edited the manuscript. AW performed bioinformatics analysis and edited the manuscript. FARN, BB, RG and AF interpreted the data and edited the manuscript. SA conceptualized and designed the study, analyzed and

interpreted the data, prepared figures and tables, and drafted and edited the manuscript. All the authors approve of the final version of the manuscript. Part of these findings were selected for Platform Presentation at the 13th International Podocyte Conference, held virtually at the University of Manchester, July 27–31, 2021 and at the ASN-APS Emerging Kidney Scientist Seminar Series, held virtually on Nov 1, 2021.

DECLARATION OF INTERESTS

The authors declare no competing interests. An Intellectual Property Application for international patent (#63/016,039) 'PPAR Agonists for Treatment of Kidney Disease' has been filed by SA and the Office of Technology Commercialization at Nationwide Children's Hospital.

INCLUSION AND DIVERSITY

While citing references scientifically relevant for this work, we also actively worked to promote gender balance in our reference list. The author list of this paper includes contributors from the location where the research was conducted who participated in the data collection, design, analysis, and/or interpretation of the work.

Received: August 26, 2021
Revised: January 2, 2022
Accepted: February 23, 2022
Published: April 15, 2022

REFERENCES

Agrawal, S., Guess, A.J., Benndorf, R., and Smoyer, W.E. (2011). Comparison of direct action of thiazolidinediones and glucocorticoids on renal podocytes: protection from injury and molecular effects. Mol. Pharmacol. *80*, 389–399. https://doi.org/10.1124/mol.111.071654.

Agrawal, S., Chanley, M.A., Westbrook, D., Nie, X., Kitao, T., Guess, A.J., Benndorf, R., Hidalgo, G., and Smoyer, W.E. (2016). Pioglitazone enhances the beneficial effects of glucocorticoids in experimental nephrotic syndrome. Sci. Rep. *6*, 24392. https://doi.org/10.1038/srep24392.

Agrawal, S., He, J.C., and Tharaux, P.L. (2021). Nuclear receptors in podocyte biology and glomerular disease. Nat. Rev. Nephrol. *17*, 185–204. https://doi.org/10.1038/s41581-020-00339-6.

Agrawal, S., Zaritsky, J.J., Fornoni, A., and Smoyer, W.E. (2018). Dyslipidaemia in nephrotic syndrome: mechanisms and treatment. Nat. Rev. Nephrol. *14*, 57–70. https://doi.org/10.1038/nrneph.2017.155.

Almeida-Oliveira, F., Leandro, J.G.B., Ausina, P., Sola-Penna, M., and Majerowicz, D. (2017). Reference genes for quantitative PCR in the adipose tissue of mice with metabolic disease. Biomed.Pharmacother. *88*, 948–955. https://doi.org/10.1016/j.biopha.2017.01.091.

Amato, A.A., Rajagopalan, S., Lin, J.Z., Carvalho, B.M., Figueira, A.C., Lu, J., Ayers, S.D., Mottin, M., Silveira, R.L., Souza, P.C., et al. (2012). GQ-16, a novel peroxisome proliferator-activated receptor gamma (PPARgamma) ligand, promotes insulin sensitization without weight gain. J. Biol. Chem. *287*, 28169–28179. https://doi.org/10.1074/jbc.M111.332106.

Aprile, M., Cataldi, S., Ambrosio, M.R., D'Esposito, V., Lim, K., Dietrich, A., Bluher, M., Savage, D.B., Formisano, P., Ciccodicola, A., and Costa, V. (2018). PPARgammaDelta5, a naturally occurring dominant-negative splice isoform, impairs PPAR gamma function and adipocyte differentiation. Cell Rep. *25*, 1577–1592.e1576. https://doi.org/10.1016/j.celrep.2018.10.035.

Araya, C.E., Wasserfall, C.H., Brusko, T.M., Mu, W., Segal, M.S., Johnson, R.J., and Garin, E.H. (2006). A case of unfulfilled expectations.Cytokines in idiopathic minimal lesion nephrotic syndrome. Pediatr.Nephrol. *21*, 603–610. https://doi.org/10.1007/s00467-006-0026-5.

Araya, C., Diaz, L., Wasserfall, C., Atkinson, M., Mu, W., Johnson, R., and Garin, E. (2009). T regulatory cell function in idiopathic minimal lesion nephrotic syndrome. Pediatr.Nephrol. *24*, 1691–1698. https://doi.org/10.1007/s00467-009-1214-x.

Awanami, Y., Fukuda, M., Nonaka, Y., Takashima, T., Matsumoto, K., Yamasaki, M., Miyazono, M., and Ikeda, Y. (2017). Successful treatment of a patient with refractory nephrotic syndrome with PCSK9 inhibitors: a case report. BMC Nephrol. *18*, 221. https://doi.org/10.1186/s12882-017-0644-0.

Buckingham, R.E., Al-Barazanji, K.A., Toseland, C.D., Slaughter, M., Connor, S.C., West, A., Bond, B., Turner, N.C., and Clapham, J.C. (1998). Peroxisome proliferator-activated receptor-gamma agonist, rosiglitazone, protects against nephropathy and pancreatic islet abnormalities in Zucker fatty rats. Diabetes *47*, 1326–1334. https://doi.org/10.2337/diab.47.8.1326.

Canetta, P.A., and Radhakrishnan, J. (2015). The evidence-based approach to adult-onset idiopathic nephrotic syndrome. Front. Pediatr. *3*, 78. https://doi.org/10.3389/fped.2015.00078.

Castoldi, E., and Rosing, J. (2011). Thrombin generation tests. Thromb.Res. *127*, S21–S25. https://doi.org/10.1016/S0049-3848(11)70007-X.

Choi, J.H., Banks, A.S., Estall, J.L., Kajimura, S., Bostrom, P., Laznik, D., Ruas, J.L., Chalmers, M.J., Kamenecka, T.M., Bluher, M., et al. (2010). Anti-diabetic drugs inhibit obesity-linked phosphorylation of PPARgamma by Cdk5. Nature *466*, 451–456. https://doi.org/10.1038/nature09291.

Choi, J.H., Banks, A.S., Kamenecka, T.M., Busby, S.A., Chalmers, M.J., Kumar, N., Kuruvilla, D.S., Shin, Y., He, Y., Bruning, J.B., et al. (2011). Antidiabetic actions of a non-agonist PPARgamma ligand blocking Cdk5-mediated phosphorylation. Nature *477*, 477–481. https://doi.org/10.1038/nature10383.

Coelho, M.S., de Lima, C.L., Royer, C., Silva, J.B., Oliveira, F.C., Christ, C.G., Pereira, S.A., Bao, S.N., Lima, M.C., Pitta, M.G., et al. (2016). GQ-16, a TZD-derived partial PPARgamma agonist, induces the expression of thermogenesis-related genes in Brown fat and visceral white fat and decreases visceral adiposity in obese and hyperglycemic mice. PLoS One *11*, e0154310. https://doi.org/10.1371/journal.pone.0154310.

de Jonge, H.J., Fehrmann, R.S., de Bont, E.S., Hofstra, R.M., Gerbens, F., Kamps, W.A., de Vries, E.G., van der Zee, A.G., te Meerman, G.J., and ter Elst, A. (2007). Evidence based selection of housekeeping genes. PLoS One *2*, e898. https://doi.org/10.1371/journal.pone.0000898.

Di Bartolo, B., Scherer, D.J., Brown, A., Psaltis, P.J., and Nicholls, S.J. (2017). PCSK9 inhibitors in hyperlipidemia: current status and clinical outlook. BioDrugs *31*, 167–174. https://doi.org/10.1007/s40259-017-0220-y.

Eddy, A.A., and Symons, J.M. (2003). Nephrotic syndrome in childhood. Lancet *362*, 629–639. https://doi.org/10.1016/S0140-6736(03)14184-0.

Fajas, L., Auboeuf, D., Raspe, E., Schoonjans, K., Lefebvre, A.M., Saladin, R., Najib, J., Laville, M., Fruchart, J.C., Deeb, S., et al. (1997). The

organization, promoter analysis, and expression of the human PPARgamma gene. J. Biol. Chem. *272*, 18779–18789. https://doi.org/10.1074/jbc.272.30.18779.

Fang, L., Zhang, M., Li, Y., Liu, Y., Cui, Q., and Wang, N. (2016). PPARgene: a database of experimentally verified and computationally predicted PPAR target genes. PPAR Res. *2016*, 6042162. https://doi.org/10.1155/2016/6042162.

Fitzgerald, K., White, S., Borodovsky, A., Bettencourt, B.R., Strahs, A., Clausen, V., Wijngaard, P., Horton, J.D., Taubel, J., Brooks, A., et al. (2017). A highly durable RNAi therapeutic inhibitor of PCSK9. N. Engl. J. Med. *376*, 41–51. https://doi.org/10.1056/NEJMoa1609243.

Floege, J., Barbour, S.J., Cattran, D.C., Hogan, J.J., Nachman, P.H., Tang, S.C.W., Wetzels, J.F.M., Cheung, M., Wheeler, D.C., Winkelmayer, W.C., et al. (2019). Management and treatment of glomerular diseases (part 1): conclusions from a kidney disease: improving global outcomes (KDIGO) controversies conference. Kidney Int. *95*, 268–280. https://doi.org/10.1016/j.kint.2018.10.018.

Friedland, S.N., Leong, A., Filion, K.B., Genest, J., Lega, I.C., Mottillo, S., Poirier, P., Reoch, J., and Eisenberg, M.J. (2012). The cardiovascular effects of peroxisome proliferator-activated receptor agonists. Am. J. Med. *125*, 126–133. https://doi.org/10.1016/j.amjmed.2011.08.025.

Gadepalli, V.S., Ozer, H.G., Yilmaz, A.S., Pietrzak, M., and Webb, A. (2019). BISR-RNAseq: an efficient and scalable RNAseq analysis workflow with interactive report generation. BMC Bioinformatics *20*, 670. https://doi.org/10.1186/s12859-019-3251-1.

Gong, H., Sun, L., Chen, B., Han, Y., Pang, J., Wu, W., Qi, R., and Zhang, T.M. (2016). Evaluation of candidate reference genes for RT-qPCR studies in three metabolism related tissues of mice after caloric restriction. Sci. Rep. *6*, 38513. https://doi.org/10.1038/srep38513.

Grahammer, F., Schell, C., and Huber, T.B. (2013). The podocyte slit diaphragm–from a thin grey line to a complex signalling hub. Nat. Rev. Nephrol. *9*, 587–598. https://doi.org/10.1038/nrneph.2013.169.

Haberman Associates (2010). Can the pharmaceutical/biotechnology industry develop better insulin sensitizers? A breakthrough result in biochemistry of PPARy. http://biopharmconsortium.com/2010/08/.

Haberman Associates (2011). Update: how the pharmaceutical/biotechnology industry might develop better insulin sensitizers. http://biopharmconsortium.com/2011/09/.

Hall, J.A., Ramachandran, D., Roh, H.C., DiSpirito, J.R., Belchior, T., Zushin, P.H., Palmer, C., Hong, S., Mina, A.I., Liu, B., et al. (2020). Obesity-linked PPARgamma S273 phosphorylation promotes insulin resistance through growth differentiation factor 3. Cell Metab. *32*, 665–675.e6. https://doi.org/10.1016/j.cmet.2020.08.016.

Heikkinen, S., Auwerx, J., and Argmann, C.A. (2007). PPARgamma in human and mouse physiology. Biochim. Biophys. Acta *1771*, 999–1013. https://doi.org/10.1016/j.bbalip.2007.03.006.

Henique, C., Bollee, G., Lenoir, O., Dhaun, N., Camus, M., Chipont, A., Flosseau, K., Mandet, C., Yamamoto, M., Karras, A., et al. (2016). Nuclear factor erythroid 2-related factor 2 drives podocyte-specific expression of peroxisome proliferator-activated receptor gamma essential for resistance to crescentic GN. J. Am. Soc. Nephrol. *27*, 172–188. https://doi.org/10.1681/ASN.2014111080.

Hunley, T.E., Ng, K.H., Smoyer, W.E., and Hidalgo, G. (2019). Pioglitazone (Pio) in Pediatric Nephrotic Syndrome (NS) (American Society of Nephrology (Kidney Week) Abstract SA-PO679), p. 939.

Kanjanabuch, T., Ma, L.J., Chen, J., Pozzi, A., Guan, Y., Mundel, P., and Fogo, A.B. (2007). PPAR-gamma agonist protects podocytes from injury. Kidney Int. *71*, 1232–1239. https://doi.org/10.1038/sj.ki.5002248.

Kerlin, B.A., Waller, A.P., Sharma, R., Chanley, M.A., Nieman, M.T., and Smoyer, W.E. (2015). Disease severity correlates with thrombotic capacity in experimental nephrotic syndrome. J. Am. Soc. Nephrol. *26*, 3009–3019. https://doi.org/10.1681/ASN.2014111097.

Kestila, M., Lenkkeri, U., Mannikko, M., Lamerdin, J., McCready, P., Putaala, H., Ruotsalainen, V., Morita, T., Nissinen, M., Herva, R., et al. (1998). Positionally cloned gene for a novel glomerular protein–nephrin–is mutated in congenital nephrotic syndrome. Mol.Cell *1*, 575–582. https://doi.org/10.1016/s1097-2765(00)80057-x.

Khoshnoodi, J., Sigmundsson, K., Ofverstedt, L.G., Skoglund, U., Obrink, B., Wartiovaara, J., and Tryggvason, K. (2003). Nephrin promotes cell-cell adhesion through homophilic interactions. Am. J. Pathol. *163*, 2337–2346. https://doi.org/10.1016/S0002-9440(10)63590-0.

Kim, D., Paggi, J.M., Park, C., Bennett, C., and Salzberg, S.L. (2019). Graph-based genome alignment and genotyping with HISAT2 and HISAT-genotype. Nat. Biotechnol. *37*, 907–915. https://doi.org/10.1038/s41587-019-0201-4.

Lee, C. (2017). Collaborative power of Nrf2 and PPARgamma activators against metabolic and drug-induced oxidative injury. Oxid. Med. Cell. Longev. *2017*, 1378175. https://doi.org/10.1155/2017/1378175.

Liao, Y., Smyth, G.K., and Shi, W. (2014). featureCounts: an efficient general purpose program for assigning sequence reads to genomic features. Bioinformatics *30*, 923–930. https://doi.org/10.1093/bioinformatics/btt656.

Luyckx, V.A., Tonelli, M., and Stanifer, J.W. (2018). The global burden of kidney disease and the sustainable development goals. Bull. World Health Organ. *96*, 414–422D. https://doi.org/10.2471/BLT.17.206441.

Ma, L.J., Marcantoni, C., Linton, M.F., Fazio, S., and Fogo, A.B. (2001). Peroxisome proliferator-activated receptor-gamma agonist troglitazone protects against nondiabetic glomerulosclerosis in rats. Kidney Int. *59*, 1899–1910. https://doi.org/10.1046/j.1523-1755.2001.0590051899.x.

Miglio, G., Rosa, A.C., Rattazzi, L., Grange, C., Collino, M., Camussi, G., and Fantozzi, R. (2011). The subtypes of peroxisome proliferator-activated receptors expressed by human podocytes and their role in decreasing podocyte injury. Br. J. Pharmacol. *162*, 111–125. https://doi.org/10.1111/j.1476-5381.2010.01032.x.

Miglio, G., Rosa, A.C., Rattazzi, L., Grange, C., Camussi, G., and Fantozzi, R. (2012). Protective effects of peroxisome proliferator-activated receptor agonists on human podocytes: proposed mechanisms of action. Br. J. Pharmacol. *167*, 641–653. https://doi.org/10.1111/j.1476-5381.2012.02026.x.

Morris, A.W. (2016). Nephrotic syndrome: PCSK9: a target for hypercholesterolaemia in nephrotic syndrome. Nat. Rev. Nephrol. *12*, 510. https://doi.org/10.1038/nrneph.2016.111.

Mukherjee, R., Jow, L., Croston, G.E., and Paterniti, J.R., Jr. (1997). Identification, characterization, and tissue distribution of human peroxisome proliferator-activated receptor (PPAR) isoforms PPARgamma2 versus PPARgamma1 and activation with retinoid X receptor agonists and antagonists. J. Biol. Chem. *272*, 8071–8076. https://doi.org/10.1074/jbc.272.12.8071.

Nakamura, T., Ushiyama, C., Osada, S., Hara, M., Shimada, N., and Koide, H. (2001). Pioglitazone reduces urinary podocyte excretion in type 2 diabetes patients with microalbuminuria. Metabolism *50*, 1193–1196. https://doi.org/10.1053/meta.2001.26703.

Nesto, R.W., Bell, D., Bonow, R.O., Fonseca, V., Grundy, S.M., Horton, E.S., Le Winter, M., Porte, D., Semenkovich, C.F., Smith, S., et al. (2003). Thiazolidinedione use, fluid retention, and congestive heart failure: a consensus statement from the American Heart Association and American Diabetes Association. October 7, 2003. Circulation *108*, 2941–2948. https://doi.org/10.1161/01.CIR.0000103683.99399.7E.

Nissen, S.E., and Wolski, K. (2007). Effect of rosiglitazone on the risk of myocardial infarction and death from cardiovascular causes. N. Engl. J. Med. *356*, 2457–2471. https://doi.org/10.1056/NEJMoa072761.

Nourbakhsh, N., and Mak, R.H. (2017). Steroid-resistant nephrotic syndrome: past and current perspectives. Pediatr. Health Med. Ther. *8*, 29–37. https://doi.org/10.2147/PHMT.S100803.

Pfaffl, M.W. (2001). A new mathematical model for relative quantification in real-time RT-PCR. Nucleic Acids Res. *29*, e45. https://doi.org/10.1093/nar/29.9.e45.

Platt, C., and Coward, R.J. (2016). Peroxisome proliferator activating receptor-gamma and the podocyte. Nephrol. Dial. Transplant. https://doi.org/10.1093/ndt/gfw320.

Radhakrishnan, J. (2020). Hypercoagulopathy in nephrotic syndrome. https://www.uptodate.com/contents/hypercoagulability-in-nephrotic-syndrome#H22.

Ritchie, M.E., Phipson, B., Wu, D., Hu, Y., Law, C.W., Shi, W., and Smyth, G.K. (2015). Limma powers differential expression analyses for RNA-sequencing and microarray studies. Nucleic Acids Res. *43*, e47. https://doi.org/10.1093/nar/gkv007.

Rovin, B.H., Caster, D.J., Cattran, D.C., Gibson, K.L., Hogan, J.J., Moeller, M.J., Roccatello, D.,

Cheung, M., Wheeler, D.C., Winkelmayer, W.C., et al. (2019). Management and treatment of glomerular diseases (part 2): conclusions from a kidney disease: improving global outcomes (KDIGO) controversies conference. Kidney Int. *95*, 281–295. https://doi.org/10.1016/j.kint.2018.11.008.

Sarafidis, P.A., Stafylas, P.C., Georgianos, P.I., Saratzis, A.N., and Lasaridis, A.N. (2010). Effect of thiazolidinediones on albuminuria and proteinuria in diabetes: a meta-analysis. Am. J. Kidney Dis. *55*, 835–847. https://doi.org/10.1053/j.ajkd.2009.11.013.

Siddall, E.C., and Radhakrishnan, J. (2012). The pathophysiology of edema formation in the nephrotic syndrome. Kidney Int. *82*, 635–642. https://doi.org/10.1038/ki.2012.180.

Sonneveld, R., Hoenderop, J.G., Isidori, A.M., Henique, C., Dijkman, H.B., Berden, J.H., Tharaux, P.L., van der Vlag, J., and Nijenhuis, T. (2017). Sildenafil prevents podocyte injury via PPAR-gamma-mediated TRPC6 inhibition. J. Am. Soc. Nephrol. *28*, 1491–1505. https://doi.org/10.1681/ASN.2015080885.

Tang, H., Shi, W., Fu, S., Wang, T., Zhai, S., Song, Y., and Han, J. (2018). Pioglitazone and bladder cancer risk: a systematic review and meta-analysis. Cancer Med. *7*, 1070–1080. https://doi.org/10.1002/cam4.1354.

Tanimoto, M., Fan, Q., Gohda, T., Shike, T., Makita, Y., and Tomino, Y. (2004). Effect of pioglitazone on the early stage of type 2 diabetic nephropathy in KK/Ta mice. Metabolism *53*, 1473–1479.

Viscoli, C.M., Inzucchi, S.E., Young, L.H., Insogna, K.L., Conwit, R., Furie, K.L., Gorman, M., Kelly, M.A., Lovejoy, A.M., and Kernan, W.N.; IRIS Trial Investigators (2017). Pioglitazone and risk for bone fracture: safety data from a randomized clinical trial. J. Clin. Endocrinol. Metab. *102*, 914–922. https://doi.org/10.1210/jc.2016-3237.

Waller, A.P., Agrawal, S., Wolfgang, K.J., Kino, J., Chanley, M.A., Smoyer, W.E., and Kerlin, B.A.; Pediatric Nephrology Research Consortium (PNRC) (2020). Nephrotic syndrome-associated hypercoagulopathy is alleviated by both pioglitazone and glucocorticoid which target two different nuclear receptors. Physiol. Rep. *8*, e14515. https://doi.org/10.14814/phy2.14515.

Wang, L., Wang, S., and Li, W. (2012). RSeQC: quality control of RNA-seq experiments. Bioinformatics *28*, 2184–2185. https://doi.org/10.1093/bioinformatics/bts356.

Weaver, D.J., Jr., Somers, M.J.G., Martz, K., and Mitsnefes, M.M. (2017). Clinical outcomes and survival in pediatric patients initiating chronic dialysis: a report of the NAPRTCS registry. Pediatr. Nephrol. *32*, 2319–2330. https://doi.org/10.1007/s00467-017-3759-4.

Yang, H.C., Ma, L.J., Ma, J., and Fogo, A.B. (2006). Peroxisome proliferator-activated receptor-gamma agonist is protective in podocyte injury-associated sclerosis. Kidney Int. *69*, 1756–1764. https://doi.org/10.1038/sj.ki.5000336.

Yang, H.C., Deleuze, S., Zuo, Y., Potthoff, S.A., Ma, L.J., and Fogo, A.B. (2009). The PPARgamma agonist pioglitazone ameliorates aging-related progressive renal injury. J. Am. Soc. Nephrol. *20*, 2380–2388. https://doi.org/10.1681/ASN.2008111138.

Yki-Jarvinen, H. (2004). Thiazolidinediones. N. Engl. J. Med. *351*, 1106–1118. https://doi.org/10.1056/NEJMra041001.

Zuo, Y., Yang, H.C., Potthoff, S.A., Najafian, B., Kon, V., Ma, L.J., and Fogo, A.B. (2012). Protective effects of PPARgamma agonist in acute nephrotic syndrome. Nephrol. Dial. Transplant. *27*, 174–181. https://doi.org/10.1093/ndt/gfr240.

STAR★METHODS

KEY RESOURCES TABLE

REAGENT or RESOURCE	SOURCE	IDENTIFIER
Antibodies		
Rabbit anti-phospho-PPARγ-Ser 273	Bioss	Cat#: BS-4888R
Rabbit anti-PPARγ	Proteintech	Cat#: 16643-1-AP; RRID: AB_10596794
Rabbit anti-GAPDH	Cell Signaling	Cat#: 2118S; RRID: AB_561053
Anti-Rabbit Peroxidase Secondary	Jackson ImmunoResearch	Cat#: 111-035-003; RRID: AB_2313567
Mouse anti-SYNPO	Santa Cruz	Cat#: sc-515842
Anti-Mouse Secondary Alexa Fluor 488	ThermoFisher	Cat#: A-11001; RRID: AB_2534069
Chemicals, peptides, and recombinant proteins		
GQ-16	Laboratory of Drs. Pitta and Neves	N/A
Puromycin aminonucleoside	Sigma-Aldrich	Cat#: P7130-100MG
Pioglitazone	Alfa Aesar	Cat#: H60507MD
Isobutylmethylxanthine	Sigma-Aldrich	CAS#: 28822-58-4
Dexamethasone	Sigma-Aldrich	CAS#: 50-02-2
Insulin	Sigma-Aldrich	CAS#: 11061-68-0
Critical commercial assays		
ACE Albumin Reagent	Alfa Wasserman	Cat#: SA2001
ACE Cholesterol Reagent	Alfa Wasserman	Cat#: SA1010
Technothrombin TGA Kit	Technoclone	Ref#: 5006010
RNeasy Kit	Qiagen	Cat#: 74104
mirVana Isolation Kit	Invitrogen	Cat#: AM1561
DNase I	Invitrogen	Cat#: 18-068-015
iScript cDNA Synthesis Kit	Bio-Rad	Cat#: 1708891
SYBR Green	Bio-Rad	Cat#: 1725121
NEBNext Ultra II Directional RNA Library Prep Kit for Illumina	New England BioLabs	Cat#: E7760L
NEBNext Poly(A) mRNA Magnetic Isolation Module	New England BioLabs	Cat#: E7490
NEBNext® Multiplex Oligos for Illumina	New England BioLabs	Cat#: 6442S/L
Luciferase Assay System	Promega	Cat#: E1500
PureLink RNA Mini Kit	Thermo Fisher	Cat#: 12183018A
ProLong Gold Antifade Mountant with DAPI	Invitrogen	Cat#: P36935
SuperBlock	Scytek	Cat#: NC1817220
Spectra Multicolor Broad Range Protein Ladder	Thermo Fisher	Cat#: PI26634
Deposited data		
RNAseq	GEO	GEO: GSE179945
Experimental models: Cell lines		
HeLa	Cell Bank of Rio deJaneiro	BCRJ code: 0100
3T3-L1 preadipocytes	Cell Bank of Rio deJaneiro	BCRJ code: 0019
Experimental models: Organisms/strains		
Rat: Wistar: Hsd:WI	Envigo	https://www.envigo.com/model/hsd-wi

(*Continued on next page*)

Continued

REAGENT or RESOURCE	SOURCE	IDENTIFIER
Oligonucleotides		
Primers	This Paper	Table S1
Recombinant DNA		
Plasmid: PPARG Ligand-Binding Domain fused to the GAL4 DNA-Binding Domain	Dr. Paul Webb, Methodist Research Institute	N/A
Software and algorithms		
ImageJ	National Institutes of Health	N/A
PPARgene Database	PPARgene	http://ppargene.org
Graphpad Prism	Graphpad software	Version 8.2.0
Picard	Broad Institute	https://broadinstitute.github.io/picard/
Ingenuity Pathway Analysis	Qiagen	N/A
MultiOntology Enrichment Tool	Medical College of Wisconsin	N/A

RESOURCE AVAILABILITY

Lead contact

Further information and requests for resources and reagents should be directed to and will be fulfilled by the lead contact, Shipra Agrawal (Shipra.Agrawal@nationwidechildrens.org).

Materials availability

This study did not generate new unique materials.

Data and code availability

- RNAseq data has been deposited at GEO and are publicly available. Accession number is listed in the key resources table.
- This paper does not report original code.
- Any additional information required to reanalyze the data reported in this paper is available from the lead contact upon request.

EXPERIMENTAL MODELS AND SUBJECT DETAILS

Animals

This study was approved by the Institution Animal Care and Use Committee at Nationwide Children's Hospital, and their guidelines were followed when performing the experiments. GQ-16 was synthesized as previously described and quality tested for 99% purity (Amato et al., 2012). Male Wistar rats (~150-200 g, 9 weeks) were intravenously (IV) injected with PAN (Sigma-Aldrich, St. Louis, MO) (50 mg/kg) on Day 0, which induced proteinuria, while control rats were given IV injections of saline. The rats were then treated by oral gavage with Pio (Alfa Aesar, Tewksbury, MA) (10 mg/kg), GQ-16 (40 mg/kg), or a sham vehicle daily. GQ-16 and Pio dosages were determined based on *in vitro* PPARγ activation, *aP2* induction and lipid accumulation data in the current study and our previous studies on the expression of thermogenesis-related genes and adipogenic effects of GQ-16 (Coelho et al., 2016) and proteinuria reducing beneficial effects by Pio (Agrawal et al., 2016). Spot urine and serum were collected, and body weights were recorded throughout the study. The rats were anesthetized with 3% isoflurane and sacrificed on Day 11, at which time blood was collected through the inferior vena cava with a 23-G needle into the 0.32% sodium citrate and 1.45 μM corn trypsin inhibitor, then processed to Platelet Poor Plasma (PPP) as described previously (Kerlin et al., 2015; Waller et al., 2020). Kidneys were harvested, and the glomeruli were isolated from 1 and ½ kidneys using the sequential sieving method (Agrawal et al., 2016). Half of the kidney was fixed in 10% buffered formalin for histologic evaluation. Cross sections of kidney containing cortex, medulla and papilla were processed routinely, sectioned at 4 μm

thickness and stained with periodic acid-Schiff method. Slides were reviewed by a pathologist blinded to the treatment method. Liver and WAT epididymal fat were collected and flash frozen in liquid nitrogen.

Cell cultures

HeLa cells were originally obtained from the Cell Bank of Rio de Janeiro. They were maintained and expanded in high glucose DMEM (Gibco, Waltham, MA) supplemented with 10% fetal bovine serum, 3.7 g/L sodium bicarbonate, 100 IU/mL penicillin, and 100 ug/mL streptomycin at 37°C and 5% CO_2. 3T3-L1 preadipocytes were maintained and expanded in high-glucose DMEM (Gibco, Waltham, MA) supplemented with 10% calf bovine serum, 3.7 g/L sodium bicarbonate, 100 IU/mL Penicillin, and 100 mg/mL Streptomycin at 37°C and 5% CO_2.

METHOD DETAILS

Urinalysis

Urine was collected from rats daily throughout the study and resolved using sodium dodecyl sulfate-polyacrylamide gel electrophoresis (SDS-PAGE) on an 8% gel and stained with Coomassie Brilliant Blue G-250 (Alfa Aesar, Tewksbury, MA) to visualize the albumin bands. All the gels were stained and developed at comparable settings. Urine protein:creatinine ratio (UPCr) analyses were performed on urine samples from Day 11 at the time of peak proteinuria by Antech Diagnostics GLP (Morrisville, NC) to quantify the proteinuria values, as previously described (Agrawal et al., 2016; Kerlin et al., 2015).

Serum chemistry

Serum albumin and cholesterol were measured using the ACE® albumin and cholesterol reagents (Alfa Wasserman Diagnostic Technologies, LLC, West Caldwell, NJ) on the Vet Axcel (Alfa Wasserman Diagnostic Technologies, LLC, West Caldwell, NJ) at the Clinical Pathology Services, The Ohio State University's College of Veterinary Medicine, according to the manufacturer's instructions.

Coagulopathy measurement

Thrombin generation assays (TGA) were performed using the Technothrombin TGA Kit (Technoclone, Vienna, Austria) and Reagent C (RC) Low on PPP samples collected from the rats to determine various parameters such as the endogenous thrombin potential (ETP) and peak thrombin concentration. These assays were performed at least in duplicate on various rat groups (n=4-7/group) as previously described (Kerlin et al., 2015). Briefly, PPP at 1:1 ratio with buffer was added to black well plates, and RC Low added. Then TGA substrate was added just before reading on a Spectramax M2 Fluorescent Plate Reader (Molecular Devices, San Jose, CA).

RNA isolation, qRT-PCR

Total RNA was extracted from isolated WAT epididymal fat and liver tissue samples using the RNeasy kit (Qiagen, Germantown, MD), following the manufacturer's instructions. Tissue samples in lysis buffer were placed in lock tubes with stainless-steel disruption beads and lysed at 30.0 Hz for 4 minutes using the Qiagen Tissue Lyser (Germantown, MD), followed by RNA isolation from the resulting lysate. Total RNA was isolated from glomeruli tissue samples using the mirVana Isolation Kit (Invitrogen, Carlsbad, CA), according to the manufacturer's instructions. Yield and purity were calculated for all isolated RNA samples by measuring the absorbance at 260, 280, and 230 nm and the ratios (both) with a spectrophotometer. 500 ng – 1 μg of RNA was subjected to DNase (Invitrogen, Carlsbad, CA) digestion at room temperature for 15 min, which was then inactivated with 25 mM EDTA at 65°C for 10 min. RNA was reverse transcribed using the iScript cDNA Synthesis Kit (Bio-Rad, Hercules, CA) according to the manufacturer's instructions. cDNA was used for quantitative reverse transcription-polymerase chain reaction (qRT-PCR) using gene specific and house-keeping primers (Table S1). SYBR green (Bio-Rad, Hercules, CA) qRT-PCR was performed on the Applied Biosystems 7500 Real-Time PCR System. The PCR conditions were 95°C for 10 min, 40 X (95°C for 15 s, 60°C for 1 min), followed by a melt curve to ensure specific products. The annealing temperature was at 60°C for all genes except *Pgc1a*, *Pparg*, and *Cd36* for which 52°C annealing temperature was used. The melt curve conditions were 95°C for 15 s, 60°C for 1 min, 30 s incremental increase to 95°C and 60°C for 15 s, as described previously (Agrawal et al., 2016). The ΔΔCt method (Pfaffl, 2001) was used to analyze the results, including normalization to housekeeping genes [*Rpl6* (deJonge et al., 2007) for glomeruli, *Ppia* (Almeida-Oliveira et al., 2017; Gong et al., 2016) for fat and liver]. Because of melt curve variation for *Trpc6*, amplified samples were also resolved on a 2% agarose gel, and densitometry was

performed using ImageJ (National Institutes of Health, Bethesda, MD) software. Each gene was tested in triplicates for each tissue on at least three different rats per group.

RNA seq, pathway analysis and ontology enrichment

For RNA sequencing, mRNA libraries were generated using ~200ng total glomerular RNA (quantified using Qubit Fluorometer) with RIN of >7, using NEBNext Ultra II Directional (stranded) RNA Library Prep Kit for Illumina (NEB #E7760L), NEBNext Poly (A) mRNA Magnetic Isolation Module (NEB #E7490) and NEBNext Multiplex Oligos for Illumina Unique Dual Index Primer Pairs (NEB #6442S/L). Libraries were sequenced with Illumina NovaSeq 6000 flow cell using paired-end 150-bp format to at least 17 million passed-filter clusters/sample (equivalent to 34 million reads). Glomerular RNA was subjected to RNA sequencing using NovaSeq6000 SP 300 cycles (=2x150bp) and using internal pipeline (Gadepalli et al., 2019), reads were aligned to Rat genome Rnor6.0 with HISAT2 (Kim et al., 2019) and counts generated for Rnor 6.0 v101 with featureCounts from the subread package (Liao et al., 2014). Post alignment quality check (QC) was assessed with fastqc, RseQC, and picard (Wang et al., 2012) (https://broadinstitute.github.io/picard). Counts were normalized with voom and differential expression tested with limma (Ritchie et al., 2015). Differential expressed genes (DEGs) were chosen with $p<0.05$ and abs(logFC)>1. Heatmaps were generated with ComplexHeatmap in R. Enriched canonical pathways were identified using Ingenuity Pathway Analysis (IPA) and GO term enrichment performed with MOET – MultiOntology Enrichment Tool [MOET, Ontology Enrichment (mcw.edu)] to identify enriched biological processes, cellular components and molecular functions.

Protein isolation, SDS-PAGE and western blotting

To isolate protein from the glomeruli, the samples were lysed in a lock tube with RIPA buffer (1 M Tris HCl, 0.5 M EDTA, 5 M NaCl, 10% SDS) containing protease inhibitor cocktail (Thermo Scientific, Waltham, MA) and phosphatase inhibitor cocktail (Alfa Aesar, Tewksbury, MA) and a stainless-steel disruption bead using a Qiagen TissueLyser (Germantown, MD). Following lysis/homogenization at 30.0 Hz for 1 min, samples were centrifuged for 10 min at 4°C at 12,000 rpm. The supernatant was collected, and the proteins and protein ladder (Spectra Multicolor Broad Range, Thermo Scientific) were resolved by SDS-PAGE and transferred to an Immobilon-P polyvinylidene difluoride (PVDF) Transfer Membrane (Millipore Sigma, St. Louis, MO). The membrane was blocked with 5% milk in phosphate buffer saline (PBS) with 0.1% Tween 20 (PBST) for 1 h, followed by incubation with the primary antibody overnight [anti-Phospho-PPARγ-Ser 273 (Bioss, Woburn, MA), anti-PPARγ (Proteintech, Carlsbad, CA), and anti-GAPDH (Cell Signaling, Danvers, MA)]. The membrane was washed three times in PBST and incubated with the secondary antibody [anti-rabbit IgG (Jackson ImmunoResearch Laboratories, Inc, West Grove, PA)] in 5% milk in PBST for 1 h. Protein bands were detected by chemiluminescence using the Chemidoc MP Imaging System (Bio-Rad, Hercules, CA). Densitometry was performed on the bands using ImageJ (National Institutes of Health, Bethesda, MD) software, and band density was subtracted from the background and normalized to GAPDH.

Immunofluorescence staining

Kidney sections were examined by indirect immunofluorescence on 3-4-micron thick paraffin sections. The sections were deparaffinized with xylene and rehydrated in graded ethanol and antigen retrieval was performed by boiling in 10 mM sodium citrate followed by washes in PBS-Tween (0.5% Tween-20). Sections were blocked with SuperBlock (Scytek Labs Inc., Logan, UT) for 6 min at 37°C, followed by incubation with anti-synaptopodin primary antibody (Santa Cruz Biotechnology) in 5% super-block at 4°C overnight at 1:100 dilution. Sections were washed with 2.5% SuperBlock in PBS-Tween (0.5% Tween-20), three times for 10 min each and incubated with fluorescent secondary antibody (Alexa Flour, 2 ug/ml; Invitrogen, Carlsbad, CA) in 5% SuperBlock in PBS for 1 hour at room temperature. Sections were washed three times for 10 min each with 2.5% SuperBlock in PBS-Tween (0.5% Tween-20) and mounted with Prolong Gold Antifade Reagent (Invitrogen). Kidney sections from the groups were viewed and imaged with equal exposures with BZ-X700 All-in-one fluorescence microscope (Keyence Inc., Itasca, IL).

PPARγ activation luciferase assay

HeLa cells were transiently co-transfected with plasmids containing human *PPARG* Ligand-Binding Domain fused to the *GAL4* DNA-Binding Domain and a plasmid containing the luciferase reporter gene under the regulation of five Gal4 DNA-binding elements (UASG× 5 TK-luciferase). These plasmids were kindly provided by Dr. Paul Webb from Methodist Research Institute, TX, USA. Transfections were conducted

using the Lipofectamine 2000 Transfection Reagent (Invitrogen, Carlsbad, CA), according to the manufacturer's instructions. Briefly, cells were plated at the density of 25,000 cells per well in 48-well plates and maintained at 37°C and 5% CO_2 for 24 h. Cells were then transfected with *hPPARG*-LBD (60 ng per well), UASG5x-Luc (240 ng per well), and pCMV-β-galactosidase (60 ng per well, used as an internal control). After 6 h, the culture medium was replaced by fresh medium containing DMSO (vehicle control) or increasing concentrations of Pio or GQ-16 (0.1 nM to 100 μM). Luciferase activity was measured using the Luciferase Assay System Kit (Promega, Madison, WI) in a luminometer (GloMax® 20/20 Luminometer – Promega, Madison, WI), following manufacturer's instructions. Results were reported as mean luciferase activity induced by the different ligands relative to vehicle control. Each experiment was performed in triplicate and repeated at least three times.

Lipid accumulation assessment and *aP2* induction

3T3-L1 preadipocytes were expanded and plated in 6-well plates for gene expression analysis (48×10^3 cells/well) or in 24-well plates for intracellular lipid accumulation assessment (12×10^3 cells/well). Two days after confluence, culture medium was switched to DMEM supplemented with 10% fetal, 100 IU/mL Penicillin, and 100 μg/mL Streptomycin, and adipose induction cocktail containing 0.5 mM isobutylmethylxanthine (Sigma-Aldrich, St Louis, MO), 250 nM dexamethasone (Sigma-Aldrich, St Louis, MO) and 1 μg/mL insulin (Sigma-Aldrich, St Louis, MO). After 72 hours, cells were maintained with DMEM containing 1 μg/mL insulin. For intracellular lipid accumulation assessment, cells were plated in 24-well plates (12×10^3 cells/well), and induced as described above, but with removal of isobutylmethylxanthine from induction medium. Vehicle control (0.1% DMSO) or ligands (100 μM pioglitazone or 100 μM GQ-16) were added throughout all adipose differentiation period. Culture medium was changed every three days, and cells were harvested 5 days after adipose induction for RNA isolation or after 10 days for lipid accumulation assessment. All experiments were conducted in triplicate.

Lipid accumulation assessment

3T3-L1 preadipocytes induced to differentiate into adipocytes were fixed in 3.7% formaldehyde. Intracellular neutral lipids were stained with Nile Red (1 μg/mL), and nucleic acid was stained with Hoechst 33342 (5 μg/mL). Relative fluorescence units (RFUs) were measured in EnSpire Multimode Plate Reader (PerkinElmer, Waltham, MA). Lipid accumulation was calculated as Nile Red RFU normalized to Hoechst RFU.

aP2 induction

RNA was isolated using PureLink RNA Mini Kit (Thermo Scientific, Waltham, MA) and its concentration and purity were assessed in a NanoVue Spectrophotometer. Quantitative real time PCR was conducted using Power SYBR green RNA-to-Ct One-Step kit (Thermo Scientific, Waltham, MA) to assess the expression of adipogenesis-related genes.

PPAR-responsive element prediction

A PPARgene database (ppargene.org) was used to predict the sequence specific PPAR-responsive elements (PPRE) on all the target genes measured in this study (Fang et al., 2016). Upon submitting the query, if the gene was predicted as a PPAR target gene, the query returned p-value and confidence level of the prediction and listed putative PPREs in the 5 kb transcription start site flanking region. Genes were assigned high-confidence category ($p > 0.8$), medium-confidence category ($0.8 \geq p > 0.6$), and low-confidence category ($0.6 \geq p > 0.45$). Genes with p value ≤ 0.45 were predicted as negative.

QUANTIFICATION AND STATISTICAL ANALYSIS

Statistics were performed using the GraphPad Prism software version 8.2.0 for Windows (GraphPad Software, San Diego, CA). Data were expressed as mean ± standard error of mean and compared using analysis of variance (ANOVA) followed by the Tukey post-hoc for grouped comparisons and Mann-Whitney test or Student's *t*-test for pairwise comparisons. Linear regression was used to quantify the correlation of measurement values using the GraphPad Prism software version 8.2.0 for Windows (GraphPad Software, San Diego, CA). *P* value significance was depicted as: * $p<0.05$, ** $p<0.01$, *** $p<0.001$, **** $p<0.0001$.